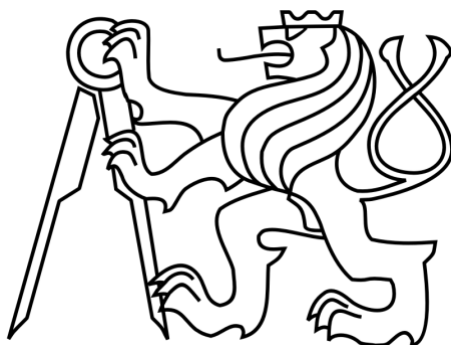# CZECH TECHNICAL UNIVERSITY IN PRAGUE

Faculty of Electrical Engineering

Department of Electromagnetic Field

MASTER THESIS

Sector slot array antenna

Sektorová anténa tvořená štěrbinami ve vlnovodu

2016   **Bc. Márton Fekete**

Supervisor: **doc. Ing. Pavel Hazdra, Ph.D.**

České vysoké učení technické v Praze
Fakulta elektrotechnická

katedra elektromagnetického pole

ZADÁNÍ DIPLOMOVÉ PRÁCE

Student: **Bc. Márton Fekete**

Studijní program: Komunikace, multimédia a elektronika
Obor: Bezdrátové komunikace

Název tématu: **Sektorová anténa tvořená štěrbinami ve vlnovodu**

Pokyny pro vypracování:

V software MATLAB vytvořte kód dle [1], který umožní návrh štěrbinové rezonanční řady v obdélníkovém vlnovodu.
Jako kritéria volte přizpůsobení, zisk a odstup postranních laloků.

Pro Vámi zvolené frekvenční pásmo navrhněte anténu s daným počtem štěrbin (volte v rozmezí 4-16) tak, aby měla a) maximální zisk b) definované potlačení postranních laloků (např. -20 dB).

Ověřte získané parametry v komerčním software FEKO resp. CST MWS.

Seznam odborné literatury:

[1] R. S. Elliot, Antenna Theory and Design, Wiley 2003

Vedoucí: doc. Ing. Pavel Hazdra, Ph.D.

Platnost zadání: LS 2016/2017

L.S.

prof. Ing. Pavel Pechač, Ph.D.
vedoucí katedry

prof. Ing. Pavel Ripka, CSc.
děkan

V Praze dne 27. 1. 2016

Čestné prohlášení

Prohlašuji, že jsem zadaný individuální projekt zpracoval sám s přispěním vedoucího práce a konzultanta a používal jsem pouze literaturu v práci uvedenou. Dále prohlašuji, že nemám námitek proti půjčování nebo zveřejňování mého projektu nebo jeho části se souhlasem katedry.

Datum: 27. 05. 2016   ……………………………………………….

                                                                    podpis

Abstrakt

Tento projekt se zabývá návrhem sektorové antény tvořené vlnovodem se štěrbinami. Sektorové antény mají vyzařovací diagram, který je široký v jedné rovině a úzký v rovině kolmé. V první části práce je analyzován vliv rozměrů štěrbiny na impedanci a rezonanční vlastnosti antén. Také je uvedeno porovnání mezi teorií a simulací. Jsou ověřeny vztahy tloušťky vlnovodu proti rezonanční vodivosti, šířky štěrbiny proti rezonanční vodivosti a délky štěrbiny proti rezonanční vodivosti. Druhá část práce se zabývá návrhovými vztahy s uvažováním vzájemných vazeb. Byly navrženy dvě antény s různou amplitudou pole a antény byly simulovány v CST Microwave Studio.

Klíčová slova: štěrbinová anténa, sektorová anténa, anténní řada ve vlnovodu, impedance štěrbiny, návrh antén, vzájemná vazba

Abstract

This thesis deals with the design of sector slot array antenna. Sector antennas have a radiation pattern which is wide in one plane and narrow in the perpendicular one. In the first part of the thesis, the effect of the slot's dimensions has been analyzed on the antenna's impedance and resonant properties. Comparison between theory and simulations is presented. The influence of waveguide wall thickness, slot width and slot length on resonant conductance is shown. The second part deals with the design equations and procedure of the slot array antennas taking the mutual coupling into account. Two antennas have been designed with different radiation patterns and they were simulated in CST Microwave Studio.

Keywords: slot antenna, sector antenna, waveguide antenna array, slot impedance, antenna design, mutual coupling

Table of Contents

List of symbols

f_c	Cutoff frequency
k	Wave number
c	Speed of light
a	Width of the waveguide
b	Height of the waveguide
Γ	Reflection coefficient
β	Phase propagation constant
λ_0	Wavelength in free space
λ_g	Wavelength in the waveguide
Z_0	Impedance of free space
G	Conductance of the slot
G_0	Characteristic conductance of the waveguide
l	Length of the slot
l_r	Resonant slot length
x	Slot offset
t	Waveguide wall thickness
N	Number of slots
V_n^s	Slot voltage of the n-th slot
V_n	Mode voltage of the n-th slot
Z_n^a	Impedance of the n-th slot
Z_n^b	Mutual coupling term
Z_{nm}	Mutual impedance of the n-th and m-th slot
g_n	Element factor
AF	Array factor

Table 1. List of important symbols

List of figures

1.   Introduction

Slot antennas are popular microwave antennas typically used at frequencies from 300 MHz to 24 GHz. They are widely used in radar navigation and as sector antennas in mobile communications. These antennas have omnidirectional radiation pattern and linear polarization. The main advantages of slot antennas are their simplicity, robustness and easy fabrication. Usually slots are used in arrays to form the desired radiation pattern and to increase the gain. The easiest way to make a slot antenna array is by cutting the slots out of the wall of a waveguide. In this case the waveguide works as a transmission line to feed the slots.

The aim of this thesis is to analyze the radiation of a longitudinal slot in the broad wall of the waveguide and examine the effect of slot dimensions and offset on the impedance of the slot and compare it to the theory. Further goals are to analyze the design equations of the slot array and to implement the design procedure in MATLAB. With the implemented code two antennas have to be made each to satisfy a different criteria.

The thesis is divided into nine main chapters. The first chapter is the introduction, it is followed by the theoretical overview, where some antenna parameters, waveguide theory and slot impedance are described. The third chapter contains the simulation results for different slot dimensions and offsets. In the fourth chapter a step-by-step guide is given to design a slot array antenna without considering the mutual coupling between the slots. Also two designed antennas and their parameters are shown in this chapter. In the fifth chapter the guide presented in chapter four is extended with the theory of mutual coupling between slots. The sixth chapter describes how the implemented MATLAB code works and the correct function of it is verified here. In the seventh chapter two antennas are presented which dimensions were calculated with the written code. The conclusion of the paper is in the eight chapter, which is followed by the list of the used sources in the last chapter.

2.   Theory

2.1.   Antenna parameters

An antenna is usually defined as the structure associated with the region of transition between a guided wave and a free-space wave or vice-versa. On transmission, an antenna accepts energy from a transmission line and radiates it into space, and on reception an antenna gathers energy from an incident wave and sends it down a transmission line [1]. In this chapter some of the main antenna parameters will be discussed.

2.1.1.   Directivity

Directivity is a measure of ability of an antenna to concentrate radiated power in a particular direction. An antenna which radiates to each direction equally is an isotropic antenna and its directivity is equal to 1. For other antennas the directivity is the ratio of the radiation intensity in that particular direction to that of isotropic antenna [2].

$$D(\Theta, \Phi) = \frac{U(\Theta, \Phi)}{\frac{1}{4\pi} P_r} \tag{1}$$

where $U(\Theta, \Phi)$ is the radiation intensity in watts per steradian and P_r is the total power radiated from the antenna:

$$P_r = \int_0^{2\pi} \int_0^{\pi} U(\Theta, \Phi) sin\Theta \, d\Theta \, d\Phi \tag{2}$$

2.1.2.   Gain

The gain of the antenna in a given direction is the amount of energy radiated in that particular direction compared to the energy an isotropic antenna would radiate in the same direction. The gain includes the power losses in the materials comprising the antenna and it is related to the directivity as follows:

$$G(\Theta, \Phi) = \eta D(\Theta, \Phi) \tag{3}$$

where η is the efficiency of the antenna and can be calculated as

$$\eta = \frac{P_r}{P_0} \tag{4}$$

P_0 is the power accepted by the antenna from the transmitter.

2.1.3.   Radiation pattern

Radiation pattern is the normalized visualization of the variation of power radiated by an antenna as a function of direction. It usually consist of a main lobe, which is in the direction of the maximum gain, and several smaller side lobes. Radiation pattern is generally 3 dimensional, however usually only 2 dimensional cuts are used in polar or Cartesian coordinate system. The main parameters of a radiation pattern are shown in Figure 1. The most important parameters are the half power beam width (HPBW) and the side lobe level (SLL).
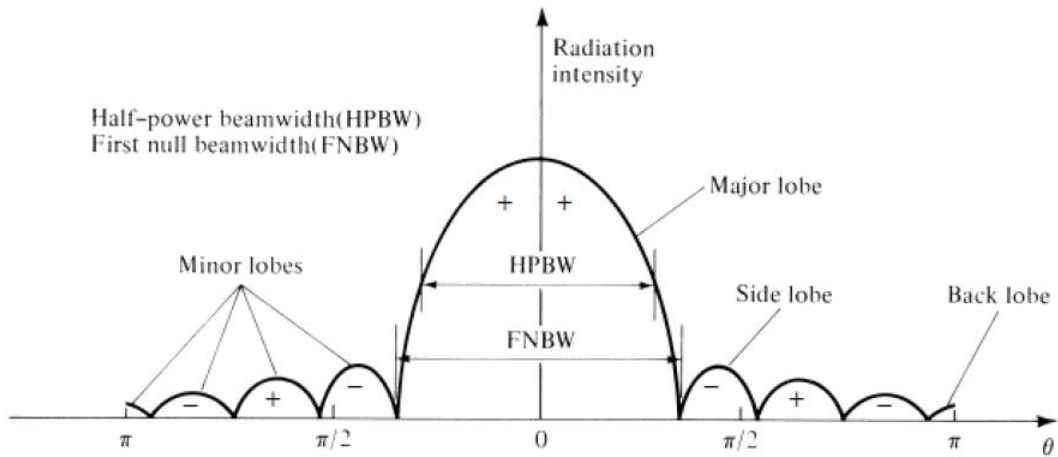
Figure 1. Radiation pattern

2.1.4. Voltage standing wave ratio (VSWR)

VSWR is a measure that numerically describes how well the impedance of the antenna is matched to the impedance of the transmission line [3]. Ideally the impedance of the antenna is matched with the impedance of the transmission line. However, perfect match is hard to achieve, therefore a small amount of energy is reflected back to the transmission line, and a standing wave is formed. VSWR is the ratio of the peak amplitude to the minimum amplitude of the standing wave. VSWR also can be calculated as follows:

$$VSWR = \frac{1 + |\Gamma|}{1 - |\Gamma|} \tag{5}$$

where Γ is the reflection coefficient, which can be calculated from the impedance of the antenna Z_A and the impedance of the transmission line Z_S:

$$\Gamma = \frac{Z_A - Z_S}{Z_A - Z_S} \tag{6}$$

9

2.2. Rectangular waveguide

A rectangular waveguide is a hollow metal pipe which is used as a transmission line connecting transmitters and receivers to antennas. They can carry high power levels while the signal attenuation is very low. Waveguides are typically filled with air, but any other dielectric material may be used.
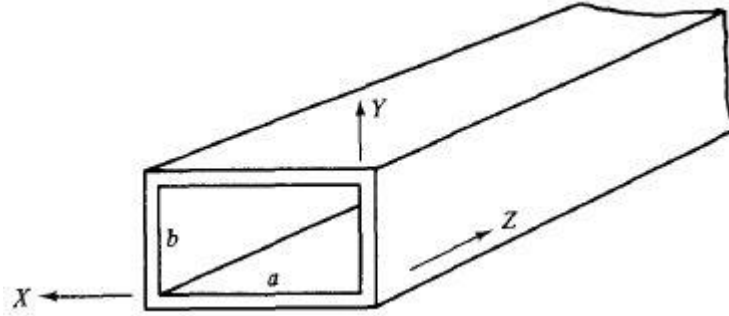

Figure 2. Rectangular waveguide [2]

Waveguides can support two different types of electromagnetic waves also referred to them as modes:

TE modes: Transverse electric modes are characterized by the fact that the electric field (E) is perpendicular to the direction of the propagation, so $E_z = 0$

TM modes: Transverse magnetic modes are characterized by the fact that the magnetic field (H) is perpendicular to the direction of the propagation and an electric field component is in the propagation direction, so $H_z = 0$

Waveguide theory often refers to these modes with *m* and *n* subscripts after them: TE_{mn} and TM_{mn}. *m* and *n* are always integers and they can take values from 0 or 1 to infinity. *m* indicates the number of half waves in the x direction and *n* is the number of half waves in the y direction.

Each mode can only propagate in the waveguide above a specific frequency, therefore waveguides also work as a high pass filter. This frequency is the cutoff frequency and it can be calculated as [4]:

$$f_c = \frac{c}{2\sqrt{\mu_r \varepsilon_r}} \sqrt{\left(\frac{m}{a}\right)^2 + \left(\frac{n}{b}\right)^2} \tag{7}$$

The dominant mode is the mode with the lowest cutoff frequency. Usually the TE_{10} mode is the dominant and in case of an air filled waveguide the previous equation simplifies to

$$f_{c10} = \frac{c}{2a} \tag{8}$$

The cutoff wave number is

$$k_c = \sqrt{\left(\frac{m\pi}{a}\right)^2 + \left(\frac{n\pi}{b}\right)^2} \tag{9}$$

and the phase propagation constant is

$$\beta = \frac{2\pi f_0}{c} \sqrt{1 - \left(\frac{f_c}{f_0}\right)^2} \tag{10}$$

where f_0 is the operating frequency.

The wavelength of the wave in the guide is different from the wavelength in free space and it is given by:

$$\lambda_g = \frac{\lambda_0}{\sqrt{1 - (f_c/f_0)^2}} \tag{11}$$

It is also important to mention that the ratio of the TE field to the ratio of the TM field for a propagation mode at a particular frequency is the impedance of the waveguide. For TE modes

$$Z_{mn}^{TE} = \frac{Z_0}{\sqrt{1 - \left(\frac{f_c}{f_0}\right)^2}} \tag{12}$$

for TM modes

$$Z_{mn}^{TE} = Z_0 \sqrt{1 - \left(\frac{f_c}{f_0}\right)^2} \tag{13}$$

where Z_0 is the impedance of free space

$$Z_0 = \sqrt{\frac{\mu}{\varepsilon}} \tag{14}$$

(a) Electric field and charge distribution   (b) Magnetic field   (c) Current flow
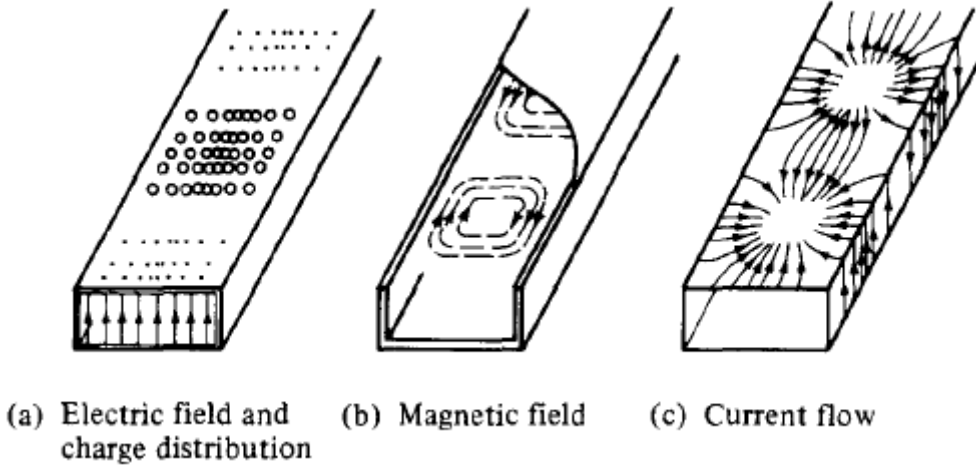
Figure 3. Field and Source Distributions for TE_{10} mode [2]

The normalized field components inside the waveguide for TE_{10} mode can be calculated from the following equations:

$$H_z = j\cos\left(\frac{\pi x}{a} e^{j(\omega t - \beta z)}\right) \tag{15}$$

$$H_x = \frac{-\beta}{\pi/a} \sin\left(\frac{\pi x}{a} e^{j(\omega t - \beta z)}\right) \tag{16}$$

$$E_y = \frac{\omega\mu}{\pi/a} \sin\left(\frac{\pi x}{a} e^{j(\omega t - \beta z)}\right) \tag{17}$$

11

2.3. Conductance of a single slot

First Stevenson published a paper about the calculation of the conductance of a slot in the broad wall of a rectangular waveguide. He used the analogy of the slot array with the transmission line to derive his results, and assumed that the slot is self-resonant. The final equation he obtained is [5]:

$$\frac{G}{G_0} = 2.09 \frac{a/b}{\beta/k} cos^2 \left(\frac{\beta}{k} \frac{\pi}{2} \right) sin^2 \left(\frac{\pi x}{a} \right) \tag{18}$$

where G is the conductance of the slot and G_0 is the characteristic conductance of the waveguide. The equation indicates that the normalized conductance of the slot is offset dependent.

Later Elliott chosen a different approach to determine the impedance of a slot, he analyzed the slot array by the field method [6]. He realized that the normalized conductance is not just offset dependent, but also changes with the length of the slot. According to him the normalized conductance of a slot can be approximated by

$$\frac{G}{G_0} = \frac{73}{R_d} \left(\frac{4 \frac{a}{b}}{0.61\pi \frac{\beta}{k}} (cos(\beta l_r) - cos(k l_r))^2 sin^2 \left(\frac{\pi x}{a} \right) \right) \tag{19}$$

where R_d is the self-resistance of the corresponding dipole and l_r is the half slot length.

For slot length $0.5\lambda_0$ the equations (18) and (19) give the same results, however for this length the slot is not resonant. As a dipole antenna should be shortened from half wavelength to make it resonant the same stands for a slot in a waveguide. According to [7] the resonant slot length is around $0.464\lambda_0$ for slot width $\lambda_0/20$ and waveguide wall thickness 1.27 mm.

3. Simulations

3.1. Simulation details

The influence of different slot parameters on normalized conductance has been analyzed. A standard R100 (WR90 according to EIA standard) waveguide has been chosen as the model of the simulation in CST Microwave Studio [8]. The recommended frequency band of this waveguide is from 8.2 GHz to 12.40 GHz, the working frequency was chosen to be at the center of this band 10.3 GHz. At this frequency the wavelength is $\lambda_0 = 29.1$ mm. The width (a=22.86 mm) and the height of (b=10.16 mm) of the waveguide remained unchanged during the simulations. The center of the slot is placed $\lambda_g/4$ from the end wall of the waveguide. This way the end wall, which is short-circuit, appears as an open-circuit and does not affect the impedance of the slot. The waveguide is fed from $\lambda_g/2$ distance from the middle of the slot, therefore the impedance of the slot is transformed to the same value in the Smith chart. The default values of the examined parameters are: thickness of the waveguide wall is set to be 0.5 mm, the slot width is $\lambda_0/20=1.455$ mm, which is according to [9] the optimal value, and the slot length is $0.464\lambda_0$ at the working frequency this means 13.5 mm. All simulations were carried out in CST.
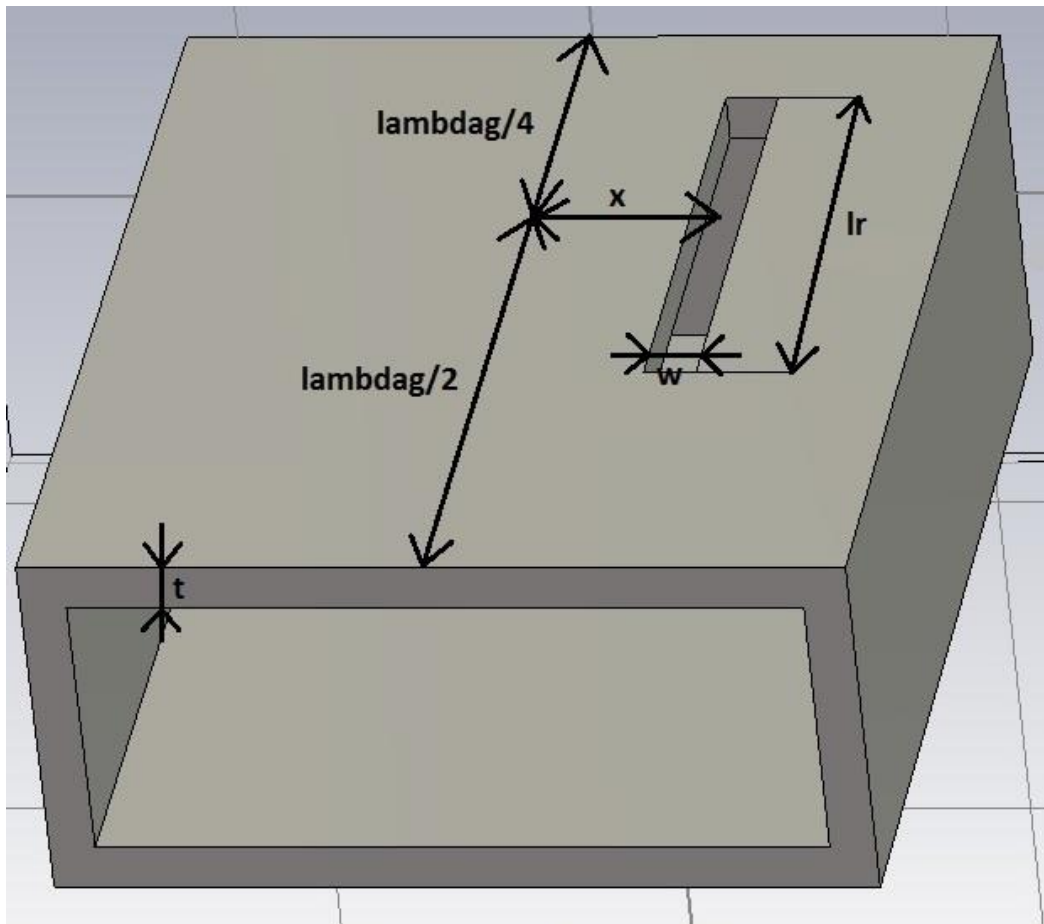

Figure 4.The model used in simulations

13

3.2. Influence of wall thickness

First the thickness of the waveguide's wall varied, including 1.27 mm which is the defined wall thickness of the R100 waveguide. For each thickness the normalized conductance has been calculated for offsets from 1 mm to 9 mm. Figure 5. shows the results compared to the theoretical curves from Stevenson and Elliott.
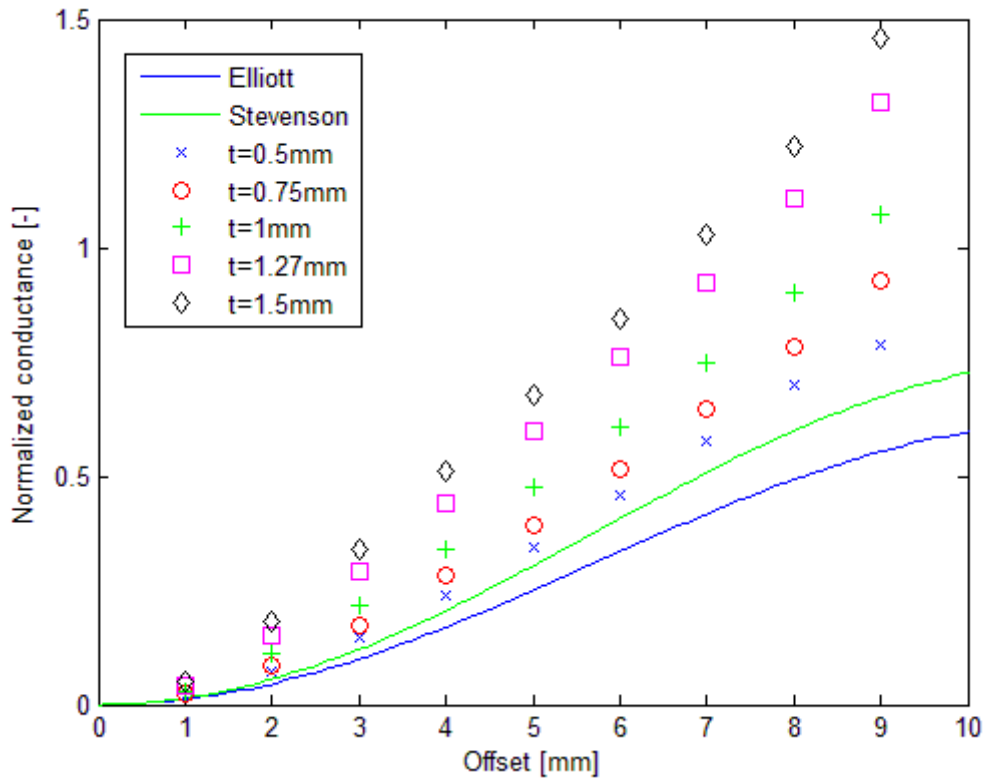

Figure 5. The influence of wall thickness on normalized conductance

Both equations have been derived for infinitely thin wall. The simulations confirm the theory, because in case of 0.5 mm wall thickness the simulated points are very close to the values calculated according to Stevenson's equation. With thicker wall the normalized conductance rises, but the shape of the curve remains similar. If we multiply the equations from Stevenson and Elliott with the correct constant the resulted curves will fit the simulated values.

With changing offset not only the conductance of the slot changes but the resonant frequency too. Although the difference is not so significant, only about 0.3 GHz between offsets 1 mm and 9 mm, we still have to keep it in mind and during antenna design modify the length of the slot accordingly. The thicker the wall of the waveguide the higher the working frequency of the slot, which means longer slot for a given frequency.
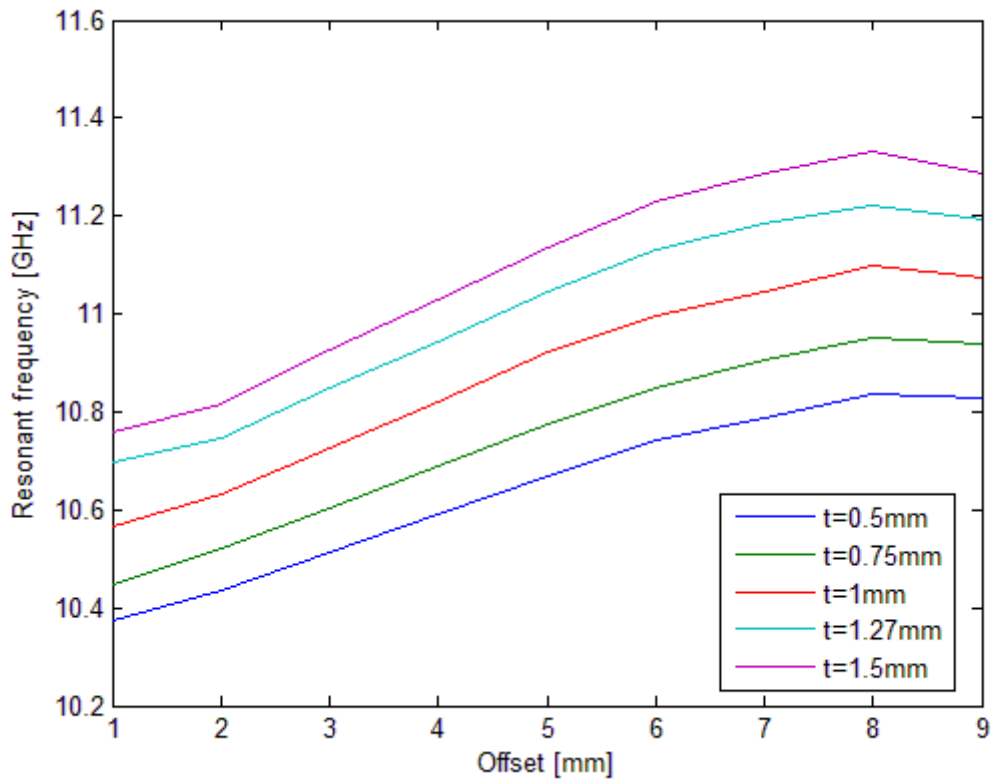
Figure 6. The influence of wall thickness on resonant frequency

3.3. Influence of slot width

Figures 7 and 8 show us the results of the simulations in which the width of the slot set to five different values. It is clearly seen that this dimension of the slot does not have a great influence on the conductance, for each width the results are nearly the same. It is also visible that the default slot width, which is 1.455 mm, is the closest to the theoretically calculated curves. Both for narrower and wider slots the conductance rises. From Figure 8 it is clear that the greater the width of the slot the higher the working frequency, however the change is so small that the influence of the width is completely negligible and no mistake is made if the recommended $\lambda_0/20$ width is used.
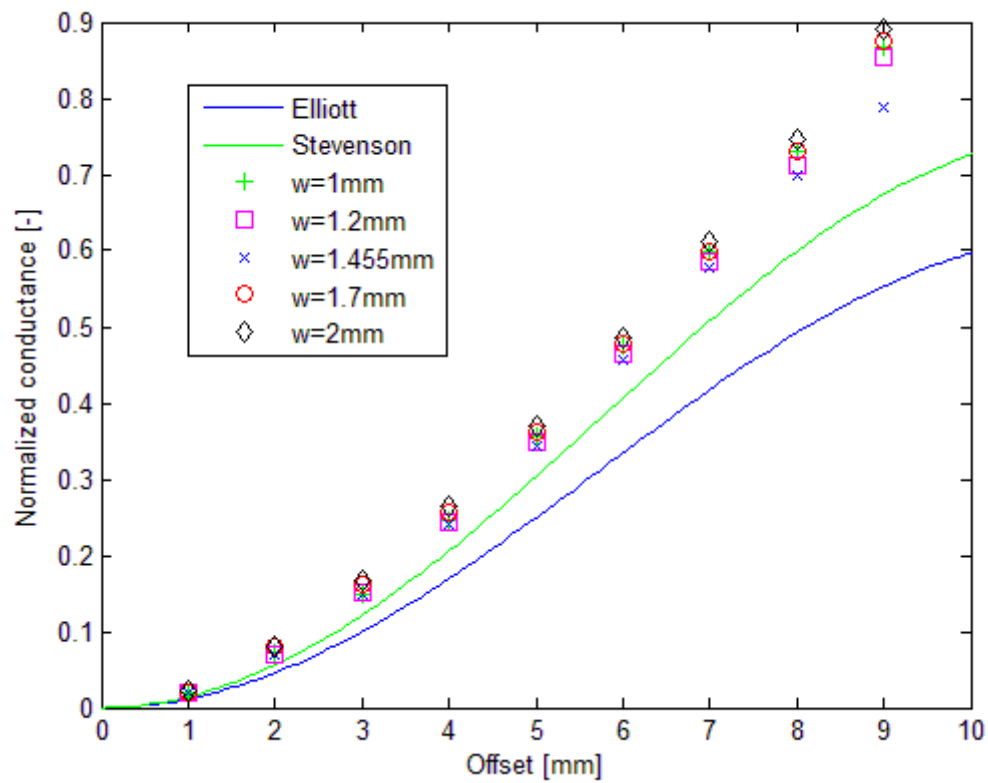
Figure 7. The influence of slot width on normalized conductance
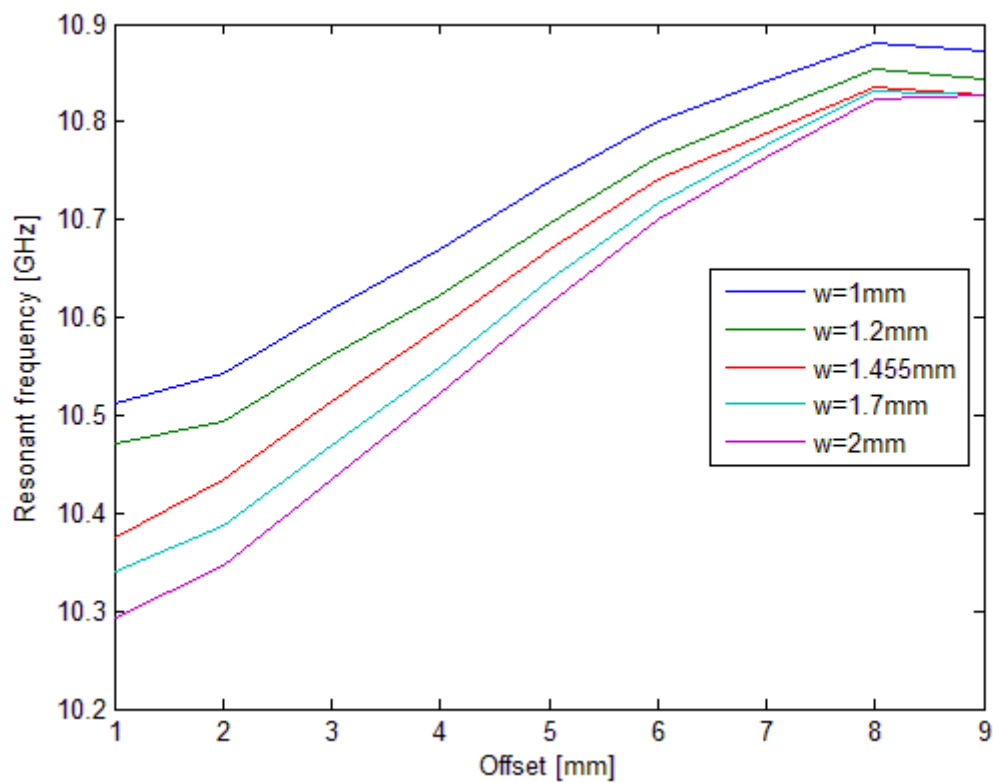

Figure 8. The influence of slot width on resonant frequency

3.4. Influence of slot length

The length of the slot is the main dimension which is used to tune the slot into resonance at a given frequency. Simulations show that with the length of the slot not only effects the resonant frequency but also the conductance of the slot. The lowest achievable conductance for each offset is for the slot length of $0.464\lambda_0$, which is in our case 13.5 mm. For this slot length the resonant frequency varies between 10.4 GHz and 10.8 GHz instead of the required 10.3 GHz, hence the slot should be longer to radiate at the desired frequency.
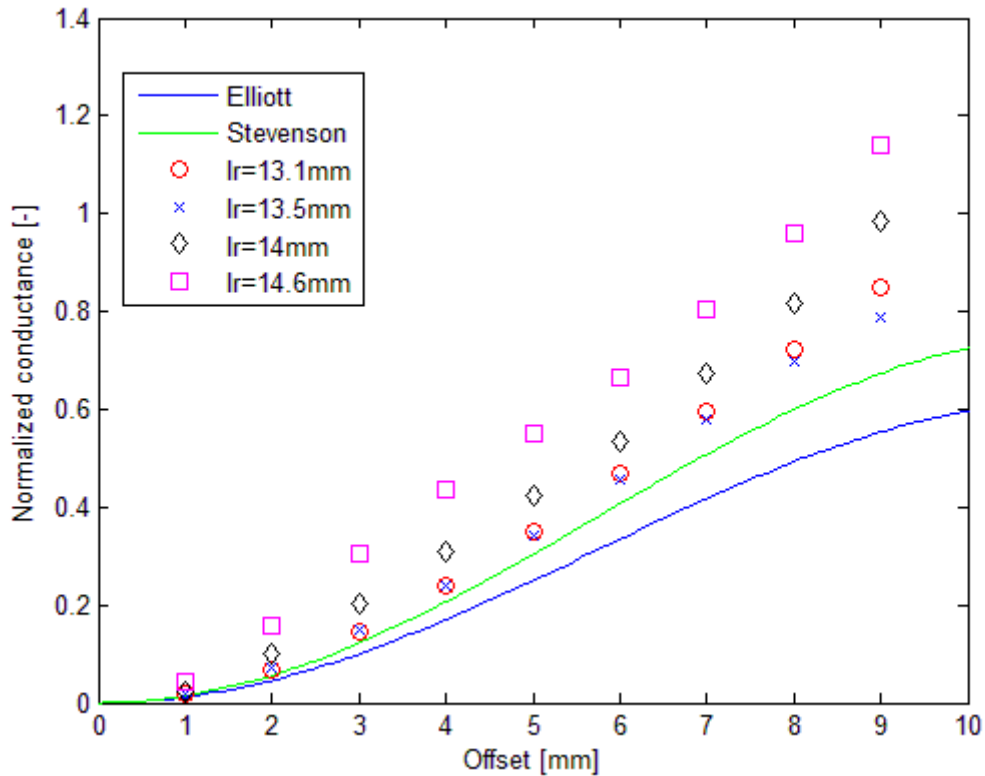

Figure 9. The influence of slot length on normalized conductance
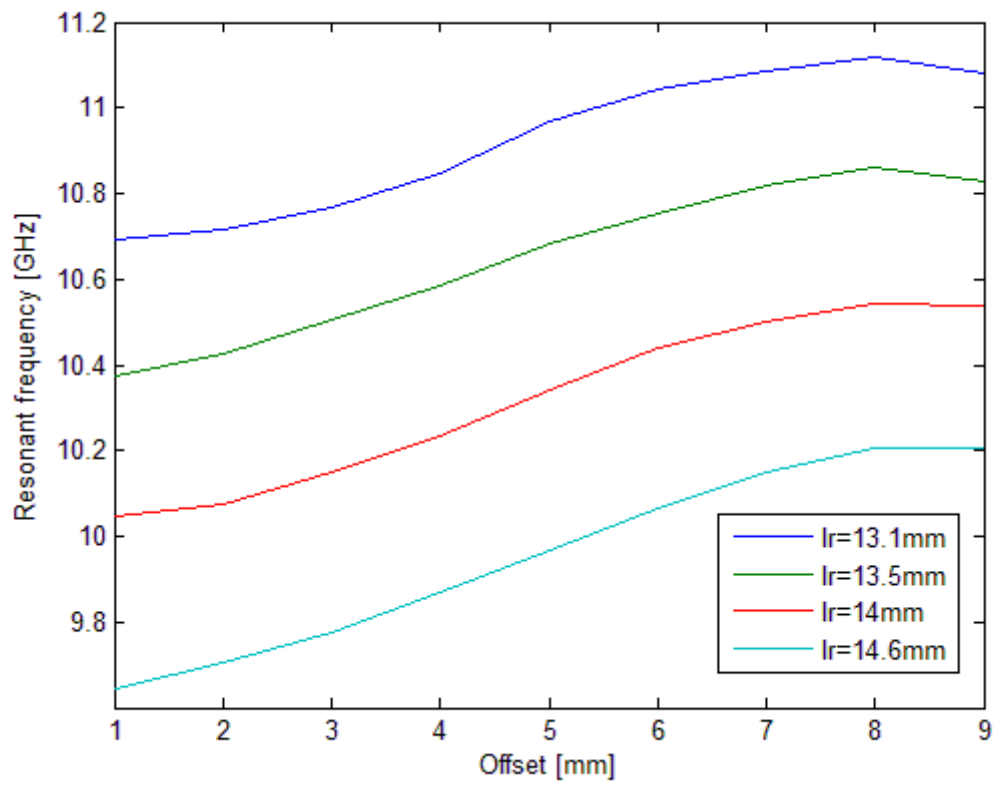
Figure 10. The influence of slot length on resonant frequency

4.   Resonant slot array design

To design a good working slot array antenna one must ensure that the slots are fed in phase. This is achieved by proper spacing between the slots. The distance between the centers of two slots should be $\lambda_g/2$ and the slots should be alternating around the center line of the broad wall of the waveguide, as shown in Figure 11. If constant amplitude distribution is required all slots must have the same offset but half of them with negative sign, otherwise the radiation pattern of the array will be inclined.
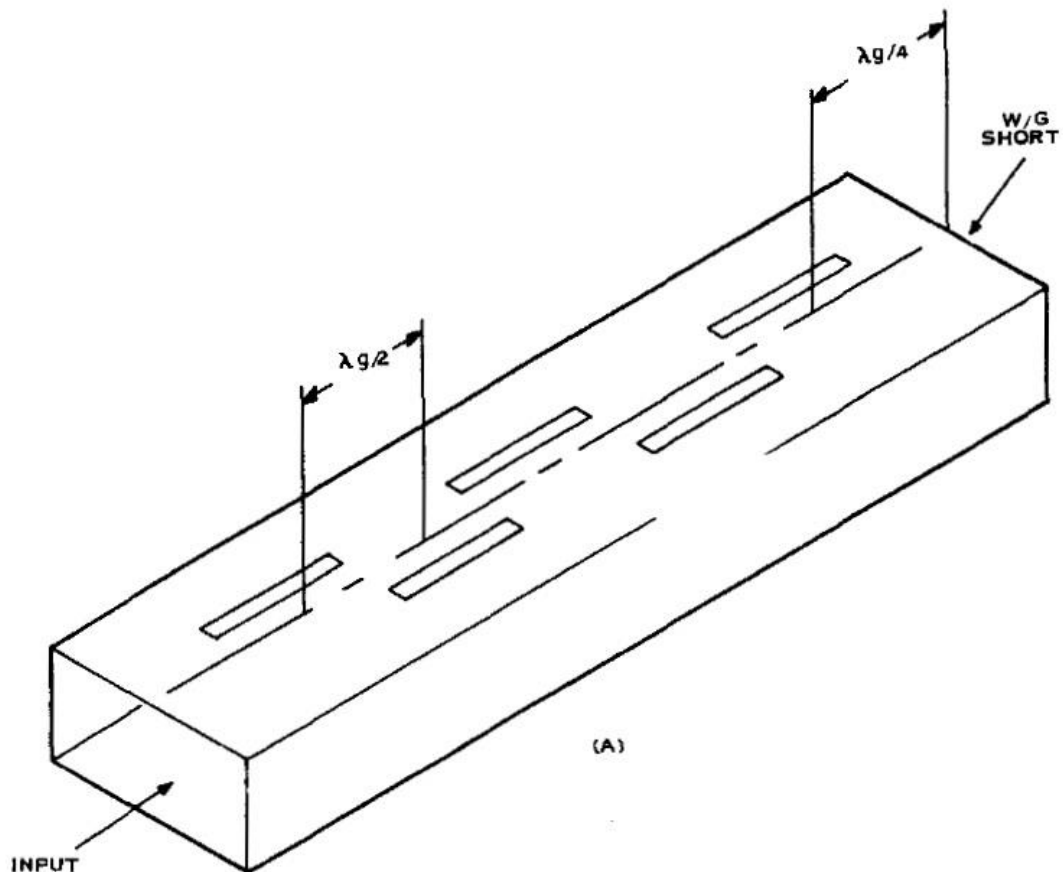
Figure 11. Resonant slot array [1]

Assuming that the slots individually are designed correctly and they are resonant their admittance is purely real. This way the slots appear as parallel admittances and we can easily calculate the input admittance of the array by adding the admittances. If the slots are identical to each other in means of offset and length, their admittance is also identical, therefore the calculation of input admittance is simplified to a single multiplication: the admittance of a single slot multiplied by the number of slots. To ensure perfect impedance matching at the input the normalized slot admittances should add up to unity, thus each slot should have an admittance of 1/N [9]. The mutual impedance between slots is not taken into consideration to make the design procedure easier.
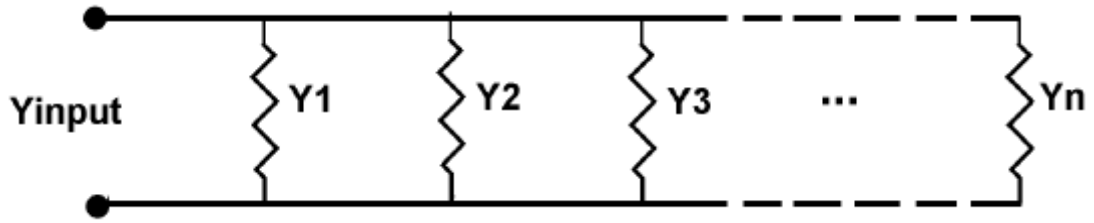
Figure 12. Circuit model of a slot array

$$Y_{input} = N * Y \qquad (20)$$

The design procedure of the slot antenna arrays were the following:

1. The required number of slots is determined
2. The normalized admittance of each slot is calculated
3. For slot length $0.464\lambda_0$ the offset is calculated from the modified equation (18) or (19)
4. Based on the simulated curves the length of the slot is tuned to resonance

With this procedure two simple antennas were modeled and simulated: a 2 slotted and a 4 slotted waveguide antenna.

4.1. Two slot waveguide antenna

Figure 13. Two slot waveguide antenna

In case of the two slot antenna the length of the slots is 14.3 mm and their offset from the center line of the waveguide is 3.19 mm. Figure 13 shows the s_{11} parameter of the antenna. At 10.3 GHz it is around -13 dB. The normalized conductance of the antenna is 1.09, it differs from the required value 1 due to the mutual impedance of the two slots.
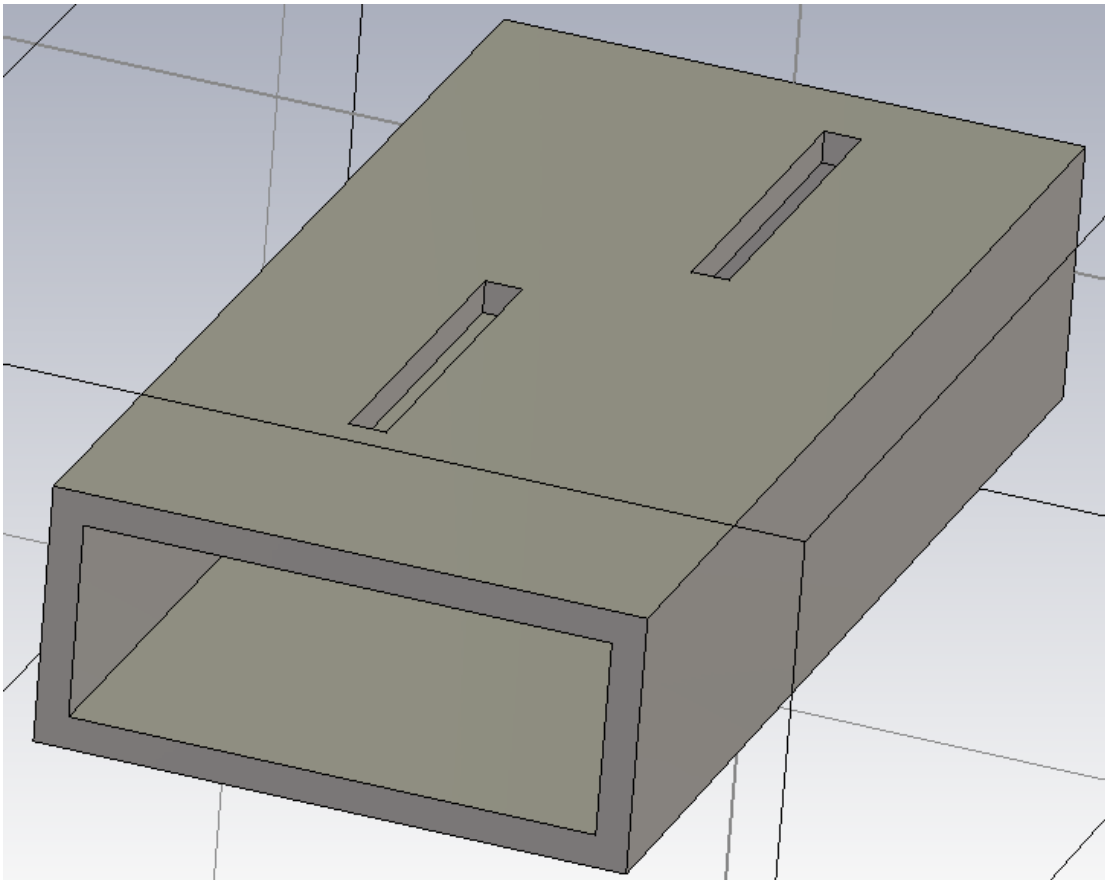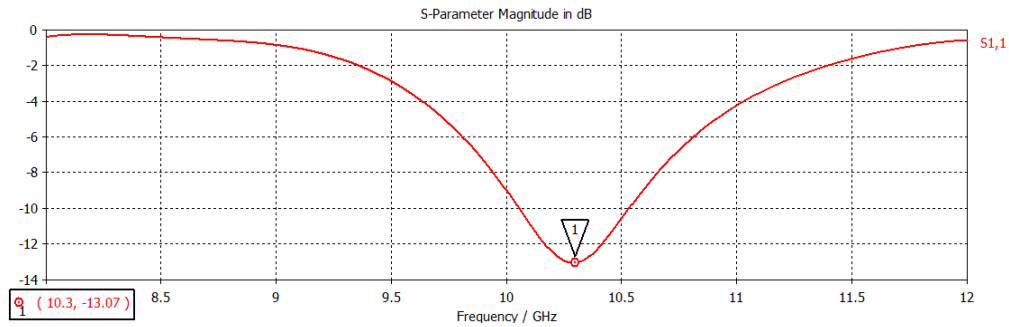

Figure 14. s11 of the 2 slot waveguide antenna

Figures 15, 16 and 17 show the radiation pattern of the antenna in 3D and in two perpendicular planes. The pattern is little inclined, not perfectly perpendicular to the slots. This is caused by the low number of the slots. Slot antenna arrays usually consist of more than two slots to shape the radiation pattern flat in one plane, however even for two slots the pattern starts to be sectorial. It is wide in one plane, the HPBW is 79.6 degrees, while in the perpendicular plane the HPBW is 39.7 degrees. The maximal gain is 9.5 dBi.
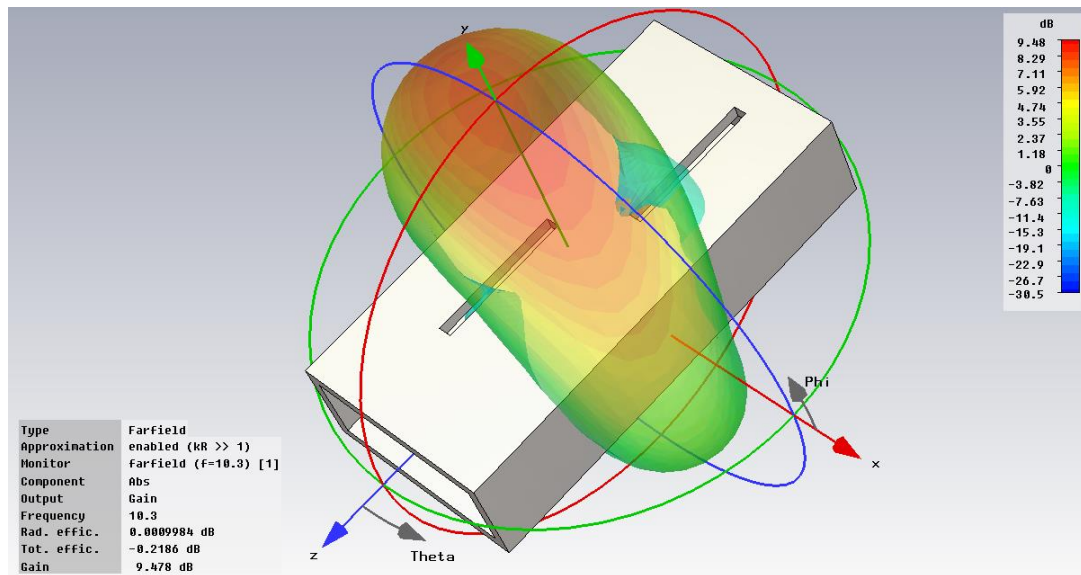
Figure 15. Radiation pattern in 3D
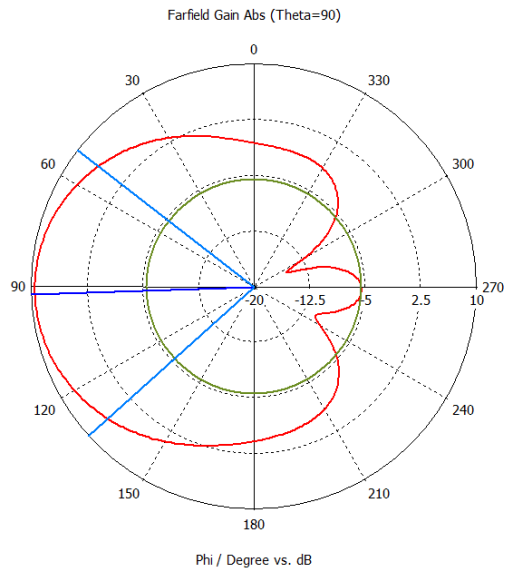
Farfield Gain Abs (Theta=90)

farfield (f=10.3) [1]

Frequency = 10.3
Main lobe magnitude =   9.5 dB
Main lobe direction =   92.0 deg.
Angular width (3 dB) =   79.6 deg.
Side lobe level = -15.0 dB

Phi / Degree vs. dB

Figure 16. Radiation pattern at theta=90°
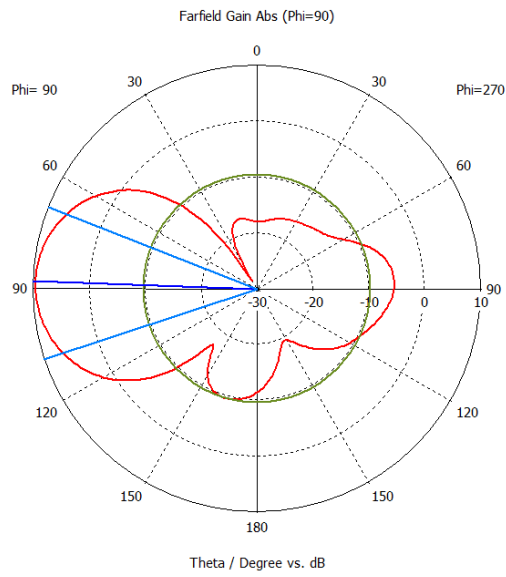
Farfield Gain Abs (Phi=90)

farfield (f=10.3) [1]

Frequency = 10.3
Main lobe magnitude =   9.5 dB
Main lobe direction =   88.0 deg.
Angular width (3 dB) =   39.7 deg.
Side lobe level = -19.1 dB

Theta / Degree vs. dB

Figure 17. Radiation pattern at phi=90°

4.2.   Four slot waveguide antenna
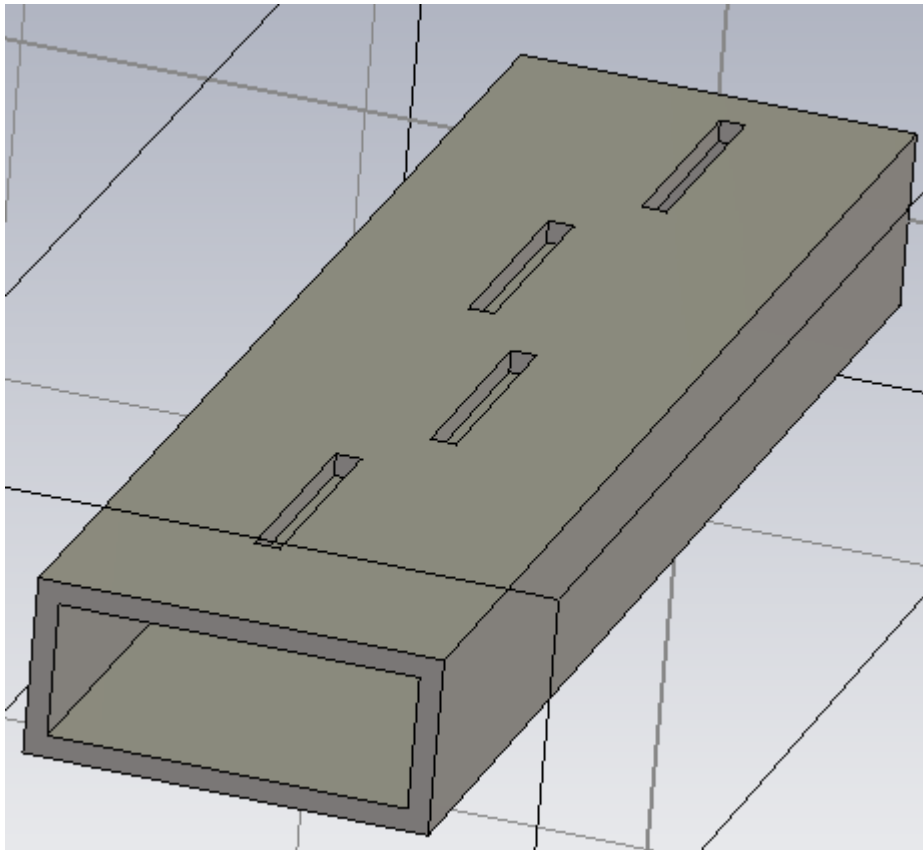
Figure 18. Four slot waveguide antenna

In case of the 4 slot waveguide antenna the slots are placed with 1.95 mm offset and their length is 14.26 mm. The resonant frequency is at 10.36 GHz and the return loss is only -5.3 dB. This is caused by the mutual impedance of the slots which is not calculated into the overall impedance during the calculations.
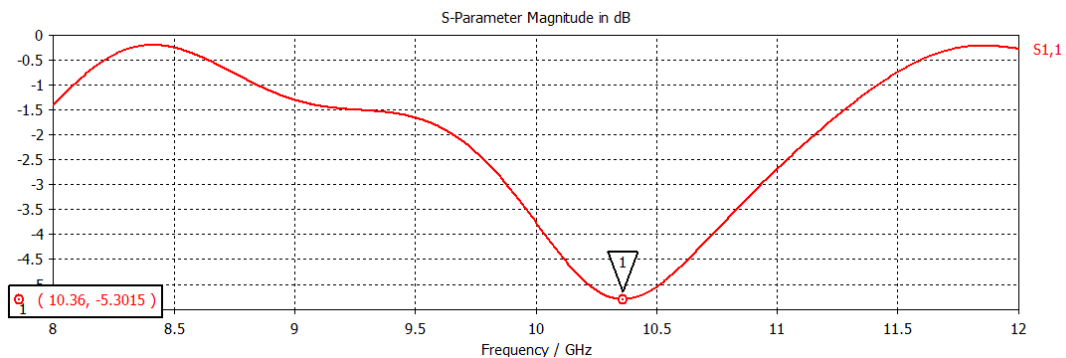
Figure 19. s11 of the 4 slot waveguide antenna

The radiation pattern of the antenna is wide only in one plane. The HPBW in the main plane is 84 degrees, in the perpendicular plane 20.4 degrees. The side lobe level is -13.1 dB, which can be improved by varying the voltage amplitude at the slots. Since the amplitude at the slots is controlled by offset, by changing the displacement we can shape the pattern to suppress the side lobes. The gain of this antenna 12.18 dBi, nearly 3 dB more than at the 2 slot array. This is correct because the number of slots has been doubled.

23

| Type	Farfield
Approximation	enabled (kR >> 1)
Monitor	farfield (f=10.3) [1]
Component	Abs
Output	Gain
Frequency	10.3
Rad. effic.	0.04713 dB
Tot. effic.	-1.493 dB
Gain	12.18 dB
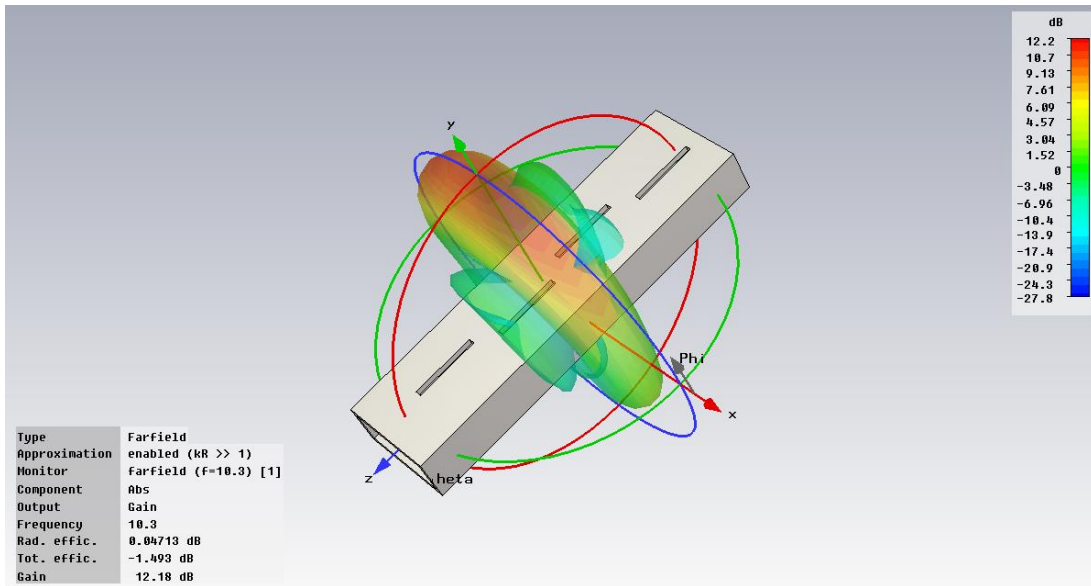
Figure 20. Radiation pattern in 3D

Farfield Gain Abs (Theta=90)

farfield (f=10.3) [1]

Frequency = 10.3
Main lobe magnitude = 12.2 dB
Main lobe direction = 92.0 deg.
Angular width (3 dB) = 84.0 deg.
Side lobe level = -13.9 dB

Phi / Degree vs. dB

Figure 21. Radiation pattern at theta=90°

Farfield Gain Abs (Phi=90)

farfield (f=10.3) [1]

Frequency = 10.3
Main lobe magnitude =   12.3 dB
Main lobe direction =   88.0 deg.
Angular width (3 dB) =   20.4 deg.
Side lobe level = -13.1 dB

Figure 22. Radiation pattern at phi=90°

5. Design equations and procedure

The two design equations developed by Elliott in [6],[10],[11] can be written as
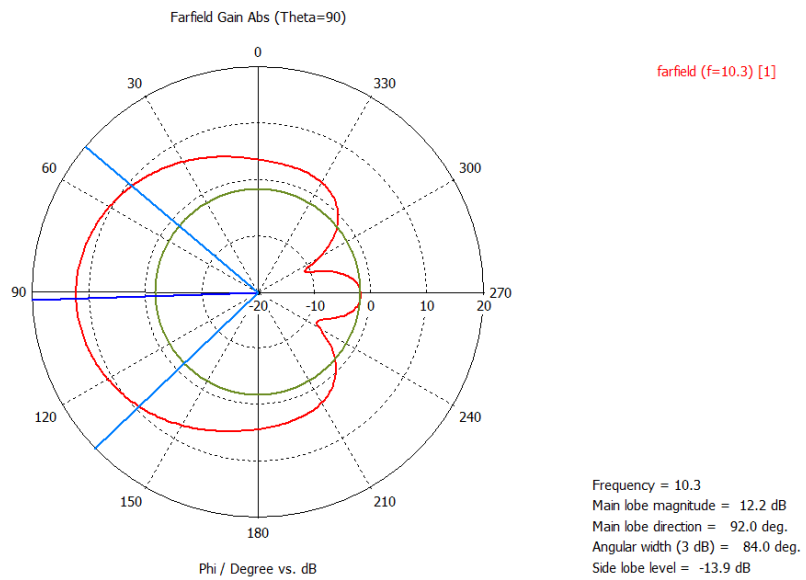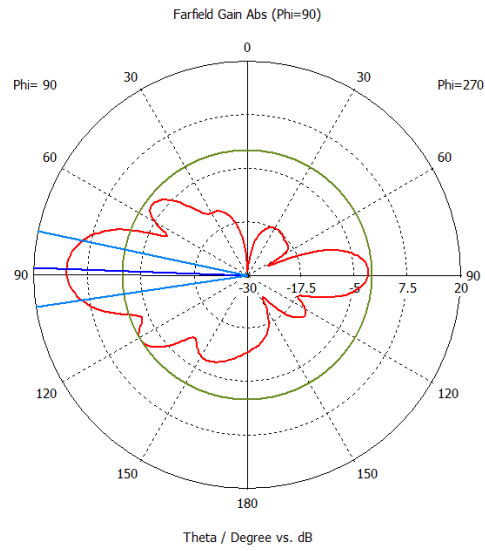
$$\frac{Y_n^a}{G_0} = K_1 f_n \sin(kl_n) \frac{V_n^s}{V_n} \tag{21}$$

$$\frac{Y_n^a}{G_0} = \frac{K_2 f_n^2}{Z_n^a} \tag{22}$$

where the constants K_1 and K_2 are

$$K_1 = -j \left[\frac{8}{\pi^2 Z_0 G_0} \frac{a/b}{\beta/k} \right]^{\frac{1}{2}} \tag{23}$$

$$K_2 = 292 \frac{\frac{a}{b}}{0.61\pi \frac{\beta}{k}} \tag{24}$$

and f_n is

$$f_n = \frac{\cos(\beta l_n) - \cos(kl_n)}{\sin(kl_n)} \sin\left(\frac{\pi x_n}{a}\right) \tag{25}$$

In equation (22) Z_n^a is the admittance of the n-th slot

$$Z_n^a = Z_{nn} + Z_n^b \tag{26}$$

and Z_n^b is the mutual coupling term calculated as

$$Z_n^b = \sum_{m=1}^{N} \frac{V_m^s \sin(kl_m)}{V_n^s \sin(kl_n)} Z_{nm} \tag{27}$$

$$Z_{nn} = Z_n + Z_n^L \tag{28}$$

Where Z_{nn} is the self-impedance of the slot and Z_{nm} is the mutual impedance of the n-th and m-th slot. Due to the slot-dipole equivalency one can assume that instead of the slots there are dipoles with corresponding length and diameter. If this assumption is made the mutual impedance between slot n=1 and m=2 may be calculated as [12]

$$Z_{21} = \frac{jZ0}{4\pi \sin(kh_1) \sin(kh_2)} \int_{-h_2}^{h_2} F(z) dz \tag{29}$$

$$F(z) = \left[\frac{e^{-jkR_1}}{R_1} + \frac{e^{-jkR_2}}{R_2} - 2\cos(kh_1) \frac{e^{-jkR_0}}{R_0} \right] \sin\big(k(h_2 - |z|)\big) \tag{30}$$

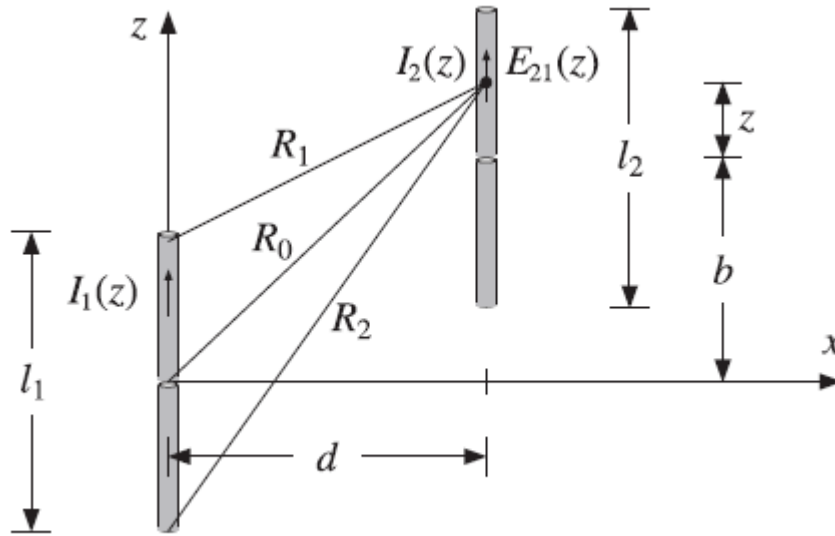Where the used values are described in Figure 23.

Figure 23. Parallel dipoles [12]

Another assumption one can make is that the input admittance of a slot is the same whether all other slots are absent or short circuited. This permits writing equations (22) and (28) in form

$$Z_{nn} = \frac{K_2 f_n^2}{Y_n/G_0} \tag{31}$$

To use the previously listed design equations the relation Y_n/G_0 versus slot length and offset has to be presented in a universal form. This may be done by poly-fitting the input data which can be obtained two ways:

1)   Constructing a series of waveguides with only one slot in each but with different offset. The offsets should vary from 0 to a/2. After Y_n/G_0 has been measured for each waveguide the length of the slot should be changed from resonant length and the measurements should be repeated. It is sufficient to make measurements in the range $0.95 l_{res} \leq l \leq 1.05 l_{res}$ Constructing and measuring this amount of waveguides can be expensive and time-consuming but electromagnetic field simulators like CST may also be used to obtain the desired data.

2)   The alternative method is solving the equation for the electromagnetic field distribution in the waveguide either via the method of moments [13] or via FDTD [14]. In these cases a correction factor may have to be used to the wall thickness and the shape of the slot.

Either method is used, the results should be the following functions:

$$h(y) = h_1(y) + jh_2(y) \tag{32}$$

$$h_1(y) = \frac{\frac{G(x,y)}{G_0}}{g(x)} \tag{33}$$

27

$$h_2(y) = \frac{\dfrac{B(x,y)}{G_0}}{g(x)} \tag{34}$$

$$y = \frac{l}{l_{res}} \tag{35}$$

$$g(x) = \frac{G_r}{G_0}(x, l_r) \tag{36}$$

$$v(x) = kl_r(x) \tag{37}$$

$$\frac{Y}{G_0} = g(x)h(y) \tag{38}$$

g(x) represents the conductance of the slot versus offset and the data is best fitted with a trigonometrical function, but higher order polynomial functions are also satisfying. v(x) gives us the resonant length versus offset. $h_1(y)$ is representing the ratio of slot conductance to resonant conductance and $h_2(y)$ gives us the ratio of susceptance to resonant conductance. Both functions are plotted versus $y = l/l_{res}$ which makes the curves offset independent. First Stegen measured this data for slots in a WR90 waveguide at frequency 9.375 GHz and his results are presented in Figures 24. to 26.
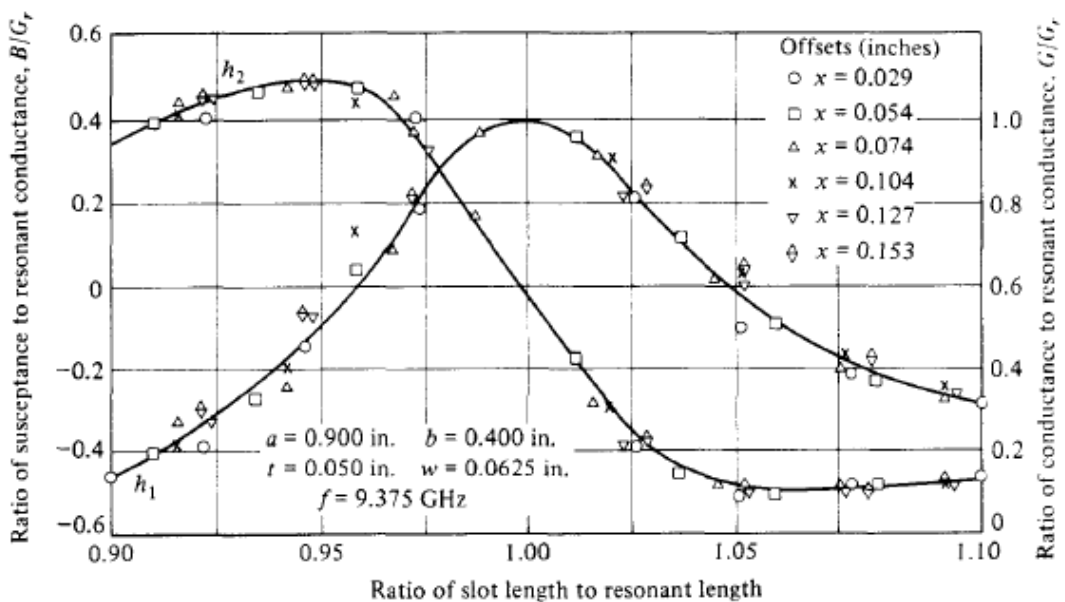
Figure 24. h1(y) and h2(y)- Normalized Self admittance component for a longitudinal slot [2]

28

Guide width a = 0.900 in.
Guide height b = 0.400 in.
Wall thickness t = 0.050 in.
Slot width w = 0.0625 in.

□ Experimental points determined by admittance measurements

○ Experimental points from radiation pattern measurements

kl_r

Slot displacement off centerline, x inches
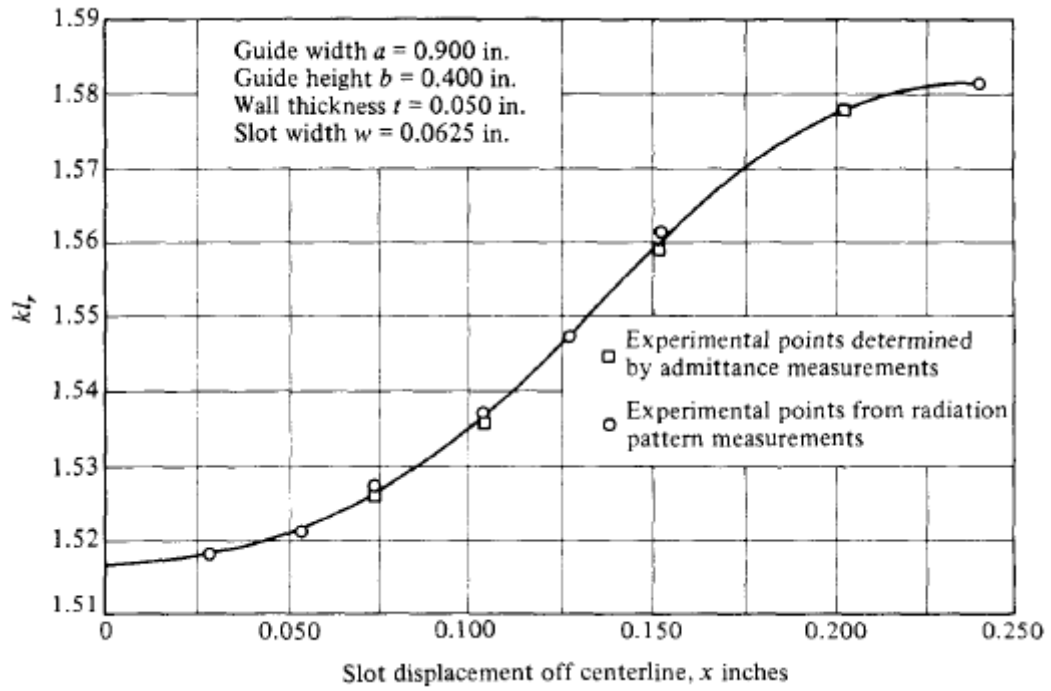
Figure 25. v(x)- Resonant length versus offset for a longitudinal slot [2]

G_r/G_0

Slot offset, x inches

Figure 26. g(x)- Normalized resonant conductance versus offset for longitudinal slot [2]

29

With equations (32)-(37) one can rewrite (31) in form

$$Z_{nn}(x_n, y_n) = \frac{K_2 f_n^2(x_n, y_n)}{g(x_n)h(y_n)}$$

(39)

and (25) as

$$f_n(x_n, y_n) = \frac{\cos\left(\frac{\beta}{k} y_n v(x_n)\right) - \cos\left(y_n v(x_n)\right)}{\sin\left(y_n v(x_n)\right)} \sin\left(\frac{\pi x_n}{a}\right)$$

(40)

Before the design procedure can be started one has to specify the slot voltage values V_n^S. As the slots are placed evenly at $\lambd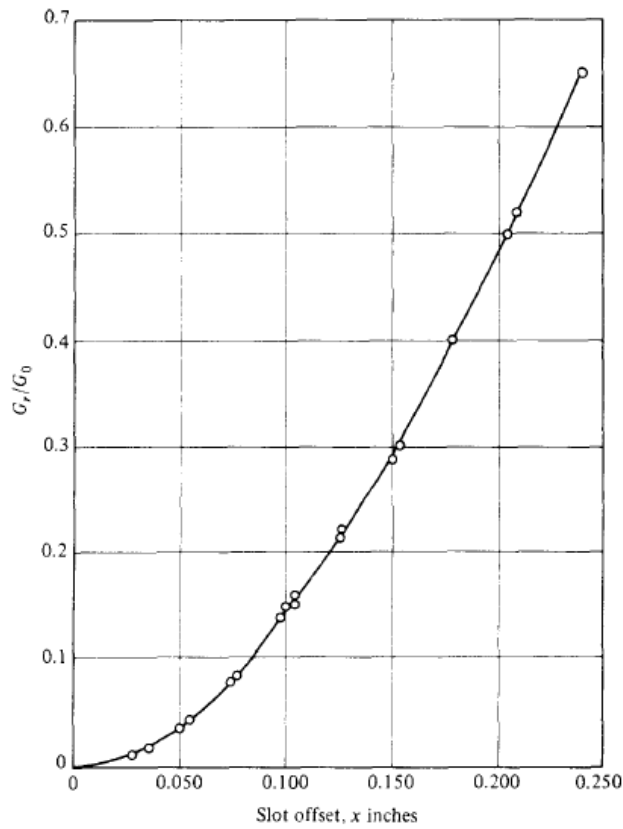a_g/2$ distances from each other, the mode voltage V_n is the same for all slots, there is only an alternation in the sign. The slot voltage values can be calculated from the required radiation pattern specifications, for example if maximal gain is requested uniform V_n^S distribution should be used through the slots. However, if a specific pattern is needed with defined first null or bandwidth or side lobe level, than V_n^S values must be calculated from the corresponding equation. A few examples are shown in Figure 27.
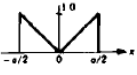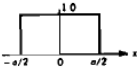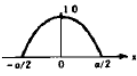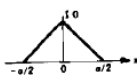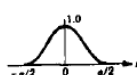
Aperture Distribution ($|x| < a/2$)	$E(x)$	$F(u)$ $u = (\pi a/\lambda)\sin\theta$	First Null (rad)	3-dB Beamwidth (rad)	Relative Gain	Side Lobe Level (dB)
	$\frac{2}{a}|x|$	$a\left(\frac{\sin u}{u} - \frac{1 - \cos u}{u^2}\right)$	$\sin^{-1}(0.75\lambda/a)$	$0.796\lambda/a$	0.742	− 4.6
	1	$a\frac{\sin u}{u}$	$\sin^{-1}(\lambda/a)$	$0.886\lambda/a$	1.0	−13.3
	$1 - (2x/a)^2$	$\frac{2a}{u^2}\left(\frac{\sin u}{u} - \cos u\right)$	$\sin^{-1}(1.43\lambda/a)$	$1.179\lambda/a$	0.833	−21.3
	$\cos(\pi x/a)$	$2\pi a\frac{\cos u}{\pi^2 - (2u)^2}$	$\sin^{-1}(1.5\lambda/a)$	$1.189\lambda/a$	⁻ 0.810	−23.1
	$1 - 2|x|/a$	$\frac{a}{2}\frac{\sin^2(u/2)}{(u/2)^2}$	$\sin^{-1}(2\lambda/a)$	$1.273\lambda/a$	0.742	−26.5
	$\cos^2(\pi x/a)$	$\frac{a}{2}\frac{\sin u}{u}\frac{\pi^2}{\pi^2 - u^2}$	$\sin^{-1}(2\lambda/a)$	$1.441\lambda/a$	0.667	−31.5

Figure 27. Radiation pattern distributions [11]

Now the design procedure can be started. The first thing to do is to calculate the initial offsets and slot lengths. This step could also be ignored and assumed that all slots are on the center line of the waveguide and have resonant length, but it is better to simple ignore the mutual coupling and calculate the slot dimensions as they were self-resonant. This way the first design equation takes the following form:

$$\frac{g_n(x)}{g_m(x)} = \frac{f_n(x_n, y_n)}{f_m(x_m, y_m)} \frac{\sin(kl_n)}{\sin(kl_m)} \frac{V_n^S/V_n}{V_m^S/V_m}$$

(41)

30

and it will insure the desired slot voltage distribution. To have an input match (42) also has to be fulfilled.

$$\sum_{n=1}^{N} g_n(x) = 1 \tag{42}$$

These equations will return the offset for all slots and the corresponding lengths can be found through function v(x).

The next step is to compute the mutual impedance between all the slots and the mutual coupling term Z_n^b. Inspecting (22) one may realize that making Y_n/G_0 pure real is only possible if the denominator is also pure real. To achieve this it is necessary to tune the slot's length from resonant length to make the slot's self-reactance compensate the reactance added with mutual coupling.

$$X_{nn} = -X_n^b \tag{43}$$

$$Im\left\{\frac{K_2 f_n^2(x_n, l_n)}{Y_n(x_n, l_n)/G_0}\right\} = -Im\{Z_n^b\} \tag{44}$$

The search for couplets x_n and l_n which satisfy equation (44) should be undertaken and it will be found that there are many possible solutions. This applies for all the slot in the waveguide. However, for a given couplet of x_n and l_n only one x_m and l_m will also satisfy the first design equation. To ensure that the right offsets and lengths have been selected the sum of active admittances must be unity, which means perfect impedance match. If this condition is not met, the procedure must be started over with a different x_n and l_n. If the sum of admittances is smaller than 1, in the next step a couplet with larger offset should be chosen, if the sum is larger than 1 than in the next iteration a smaller offset should be selected.

After the right offsets and lengths have been found the process from calculating the mutual impedances has to be iterated, because the new values can be used to compute an improved Z_n^b from which a better offset and length combination can be found. The iterations should be continued until the difference between two steps is smaller than the defined tolerance. The process converges quickly, usually only a few iterations are needed.

The radiation pattern of the slot array may be calculated as derived in [15],[16]:

$$F(\Theta) = \sum_{n}^{N} \left|\frac{V_n^s}{V_1^s}\right| g_n(\Theta) AF(\Theta) \tag{45}$$

where $g_n(\Theta)$ is the element factor of a slot, and it is derived by assuming an equivalent dipole with length *l*

$$g(\Theta) = \frac{\cos(kl \cos(\Theta)) - \cos(kl)}{\sin(\Theta)} \tag{46}$$

and $AF(\Theta)$ is the array factor for the linear array with z_n as the position of the n-th slot

$$AF(\Theta) = e^{j(z_n k \cos(\Theta))} \tag{47}$$

6. MATLAB code realization

Based on the design procedure described in the previous chapter a MATLAB code has been written. To present how it works and to test its correctness a simple 4 slot array is designed, the same which is described in [2]. The requirements for this antenna were perfect input match and an array specification which is achieved with the slot voltage distribution ratio of 1:2:2:1, but obviously the code works for arbitrary number of slots and voltage distribution.

For convenience a standard WR-90 waveguide is chosen and the working frequency of 9.375 GHz, this way Stegen's curves can be used [17]. These curves are the main input parameters and are loaded as two vectors each: one vector represents the x values of the curve and the second the y values. The polyfits to the curves are gain using the inbuilt *fit* function of MATLAB. For *g(x)* a sixth order polynomial fit is used because for lesser grade polynomial functions the results were completely off. The other curves are represented with a quadratic equation.

Now we have to solve equations (41) and (42) simultaneously to get the initial offset values. To do this the function *fsolve* has been used. The input parameters for *fsolve* work also as the starting values, for which values this solver begins the calculation. Unfortunately the fitted curve expressions can't be used as an input parameter, therefore first they are saved to a correspondingly named file, which are loaded later in the function. The two equations has to have the form of *fun(x)=0*, otherwise MATLAB is not able to solve them. Another interesting observation was made, this one regarding the slot voltage distribution. If the voltage distribution is uniform, which means all the offsets and length are the same, (41) becomes unusable as arbitrary offset will satisfy it. Therefore for uniform voltage distribution a different function is used, which is only based on equation (42). In both cases a vector of offsets is the returned results. Although all the values are positive, one will have to keep in mind that the slots have to alternate around the center line of the waveguide. The slot lengths are calculated from the offsets with function v(x).

The starting offsets and the normalized slot lengths according to Elliott and the calculated ones are presented in Table 2. Since the slot voltage distribution is symmetrical slot 1 and 4 and slots 2 and 3 have same dimensions.

	Elliott		Calculated	
Slot	Offset [mm]	2l/λ [-]	Offset [mm]	2l/λ [-]
1	2,0828	0,487	2,0946	0,4868
2	4,5720	0,502	4,5654	0,5017
3	4,5720	0,502	4,5654	0,5017
4	2,0828	0,487	2,0946	0,4868

Table 2. Starting lengths and offsets

Both cases have been simulated in CST and the difference is presented in Figure 28. and 29. As it can be seen the difference between the two cases is negligible. Surprisingly the antennas are better matched at frequency around 10.4 GHz which may be caused by the fact that the Stegen curves were measured for round cornered slots. There is no information presented in [17] about the exact roundness of the slots, therefore rectangular slots have been used during the simulations.
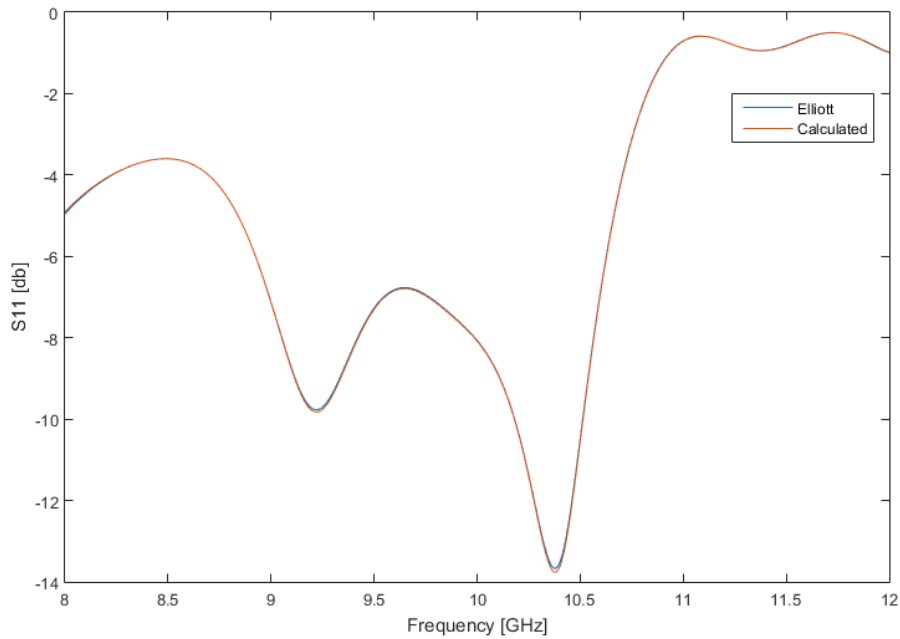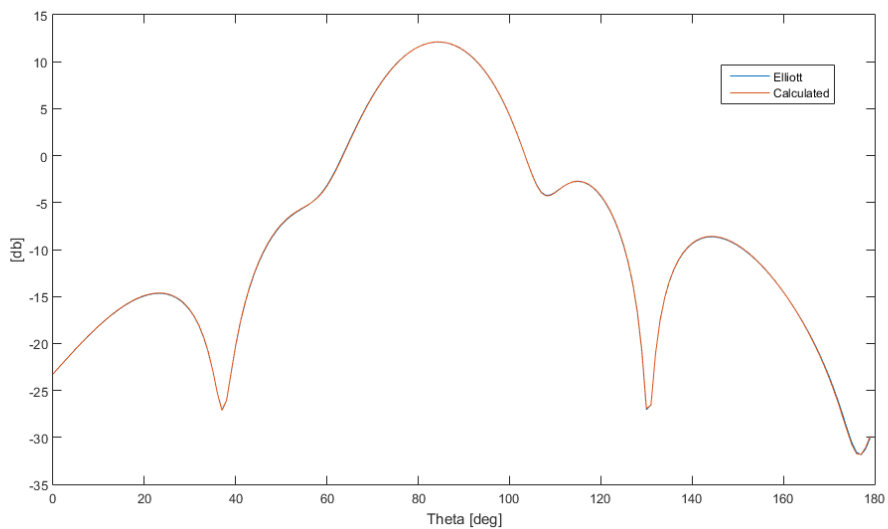
Figure 28. s11 parameter of antennas

Figure 29. Radiation pattern at 9.375 GHz

The radiation patterns are identical, but the whole pattern is inclined. The maximum is at Θ=85° which causes that the first side lobe around Θ=55° is partially part of the main lobe. The pattern is also asymmetrical as the side lobes at Θ=120° and at Θ=145° have a greater magnitude. The gain of the antennas is 12 dB and the side lobe level ratio is 13.1 dB.

With the assumed starting lengths and offsets the mutual impedances may be calculated according to (29) and (30). These equations are already implemented in the Electromagnetic Waves and Antennas toolbox [12] as function *imped* originally for dipoles with length *l* and diameter *a* with side-by-side distance of *d* and collinear offset of *b.* However, as described before due to the slot-dipole equivalency it can be used for slots

too. It is worth mentioning that all inputs are in proportion to wavelength. The calculated Z_{nm} values are:

	Elliott	Calculated
Z12	0,37-j8,39	0,3632-j8,3944
Z13	1,49+j1,28	1,4858+j1,2793
Z14	-0,67+j0,47	-0,6699+j0,4730
Z23	-2,88-j7,81	-2,8448-j7,991

Table 3. Mutual impedances

From these values the initial mutual coupling term Z_n^b for slots are computed as written in (27):

$$Z_1^b = \frac{V_2^s \sin(kl_2)}{V_1^s \sin(kl_1)}(Z_{12} + Z_{13}) + \frac{V_1^s \sin(kl_1)}{V_1^s \sin(kl_1)}Z_{14} = 3.0312 - j13.7692 \tag{48}$$

$$Z_2^b = \frac{V_1^s \sin(kl_1)}{V_2^s \sin(kl_2)}(Z_{13} + Z_{12}) + \frac{V_2^s \sin(kl_2)}{V_2^s \sin(kl_2)}Z_{23} = -1.9211 - j11.3537 \tag{49}$$

Since the objective is to make Y_n^a/G_0 pure real we have to find the couplets of x_1, y_1 and x_2, y_2 which satisfy (44) in form of

$$Im\left\{\frac{K_2 f_1^2}{g(x_1)h(y_1)}\right\} = -Im\{Z_1^b\} = 13.7692 \tag{50}$$

$$Im\left\{\frac{K_2 f_2^2}{g(x_2)h(y_2)}\right\} = -Im\{Z_2^b\} = 11.3537 \tag{51}$$

and also satisfy the pattern restriction written as

$$\frac{Y_2^a/G_0}{f_2 V_2^s \sin(y_2 v(x_2))} = \frac{Y_1^a/G_0}{f_1 V_1^s \sin(y_1 v(x_1))} \tag{52}$$

and the couplets should also achieve perfect input admittance match

$$\sum_{n=1}^{N} \frac{Y_n^a}{G_0} = 1 \tag{53}$$

Equations (50) through (53) are solved in MATLAB using a numeric solver function, namely *vpasolve*. First x_1, y_1 and x_2, y_2 values are calculated from (50) and (51) and checked if they satisfy (53). If not, new values are chosen as there are more possible solutions for both equations. If the perfect pair is found the written function also checks if the condition in (52) is met. Just as before if not the search for different values should be continued.

The found result are presented in Table 4. The calculated values are nearly the same as Elliott's offsets and lengths. As it can be seen the admittances Y_n^a/G_0 are pure real and they sum up to 0.9894, which is nearly a perfect match. Comparing the initial and the recalculated values shows that there is only a 1-1.5% change in the offsets and the lengths. The process could be iterated but the new values would be so close to the current one that it would not have any effect on the radiation pattern or on the impedance match.

	Elliott				Calculated			
Slot	Offsets [mm]	2l/λ [-]	y [-]	Y/G0	Offsets [mm]	2l/λ [-]	y [-]	Y/G0
1	2,1844	0,4933	1,0125	0,0988	2,0711	0,4929	1,0126	0,0882
2	4,4704	0,5058	1,0099	0,4010	4,5262	0,5064	1,0099	0,4065
3	4,4704	0,5058	1,0099	0,4010	4,5262	0,5064	1,0099	0,4065
4	2,1844	0,4933	1,0125	0,0988	2,0711	0,4929	1,0126	0,0882

Table 4. Final offset and length values

Figure 30. shows the s_{11} parameter of the improved antennas compared to the one with the initial parameters. As visible the calculation with mutual coupling has worsen s_{11} at the desired frequency and the best impedance match is still at 10.4 GHz. This may be caused by the inaccuracy of the used Stegen curves.
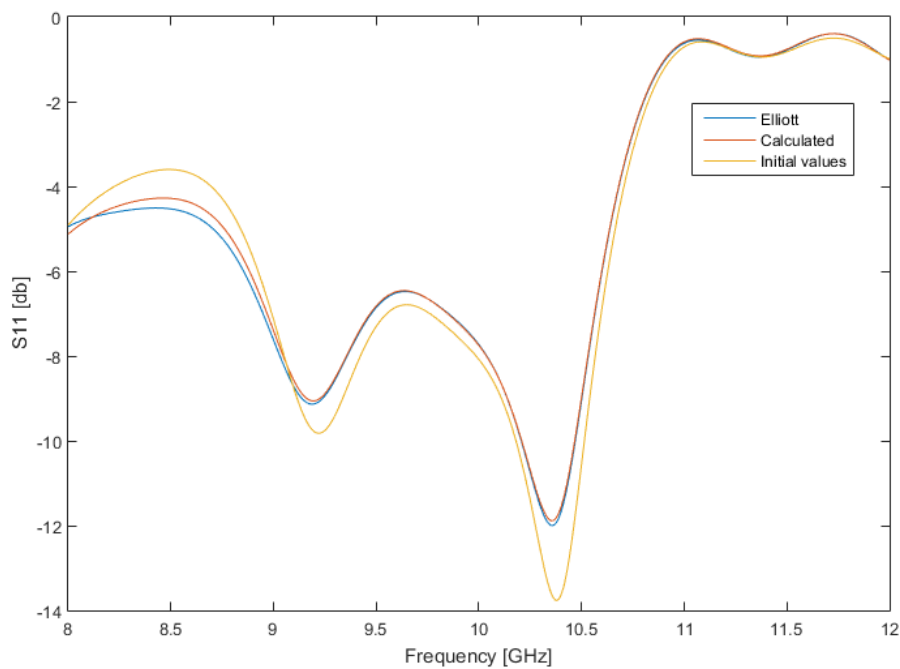

Figure 30. s11 parameter of the antennas

In Figure 31. the radiation patterns are compared with the theoretical curve. Unfortunately the improved values of offsets and lengths did not improve the radiation pattern of the antenna, it has even worsen the side lobe level ratio by 2dB. It is clearly visible that the simulated pattern is inclined by 5 degrees, the main lobe's direction is at Θ=85° but according the theory the maximum should be at Θ=90°. Also the main lobe is much wider than the theoretically calculated, the first nulls have disappeared from the pattern as the main lobe and the first side lobes merged.
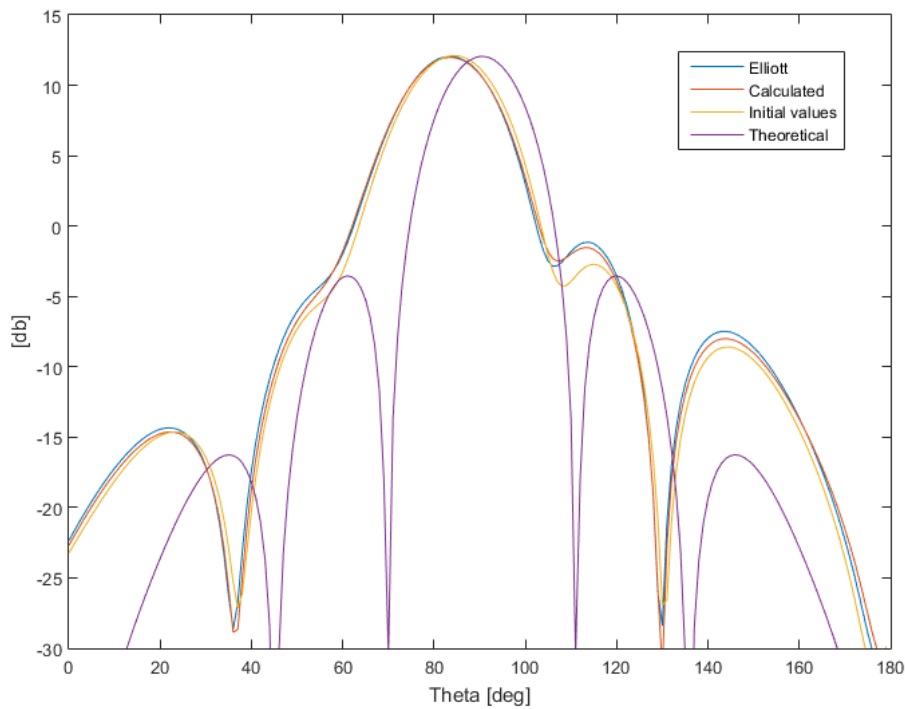
Figure 31. Radiation pattern of the antennas

7. Designed antennas

Using the MATLAB code two antennas have been designed, both at frequency 10.2 GHz. To ensure the accuracy of the antennas a series of simulations were carried out in CST at this frequency for various slot offset and length and from the results the four curves g(x), v(x), h1(x) and h2(x) have been reconstructed. These four curves were the main input data for the calculation. Both antenna arrays consist of 8 slots.

7.1. Maximal gain antenna

The first antenna was made with the intention to achieve the maximum gain possible, therefore the slot voltage is the same for each slot. The initial offset values were found to be 2.4154 mm and the corresponding slot length is 15.62 mm. With the calculation of mutual impedances the offsets and lengths have improved to the values presented in Table 5:

Slot	1	2	3	4	5	6	7	8
Offsets [mm]	2,4015	2,3866	2,3885	2,3893	2,3893	2,3885	2,3866	2,4015
Length [mm]	15,721	15,827	15,813	15,807	15,807	15,813	15,827	15,721

Table 5. Slot dimensions of the maximal gain antenna

Figure 32. perfectly illustrates the effect of the mutual coupling. Without it the s_{11} parameter of the antenna at 10.2 GHz is 20 dB worse than in case when the mutual impedance of the slots was considered. Surprisingly the antenna is matched at 2 frequencies, at the desired 10.2 GHz and also at 9.15 GHz.
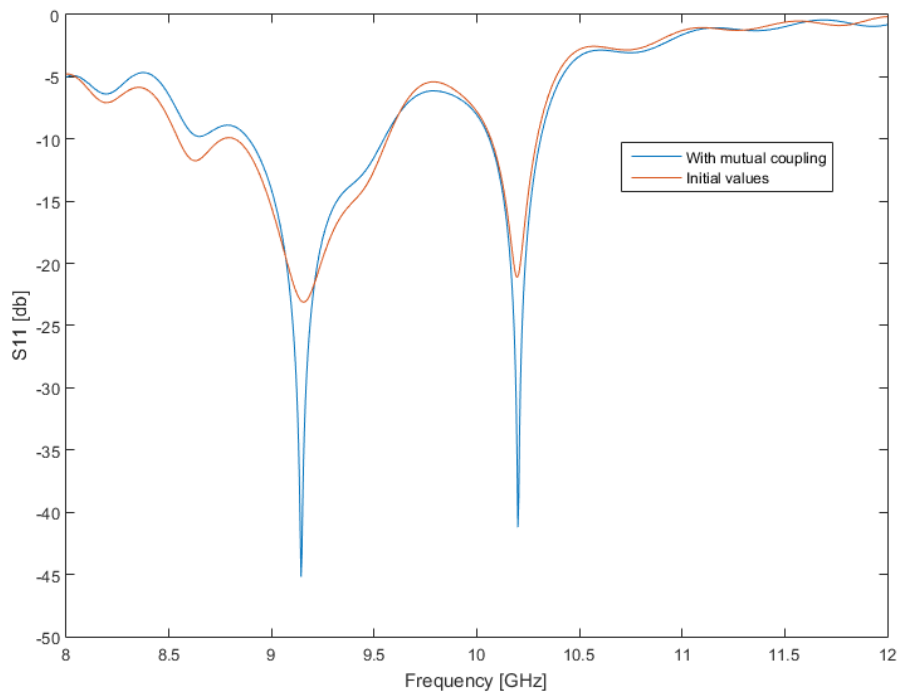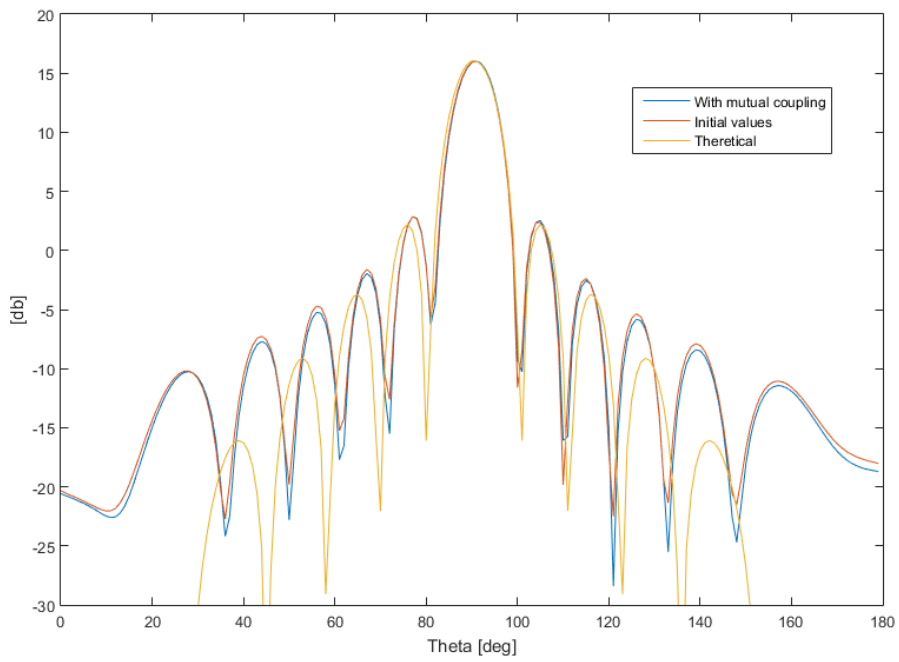
Figure 32. s11 parameter of the maximal gain antenna

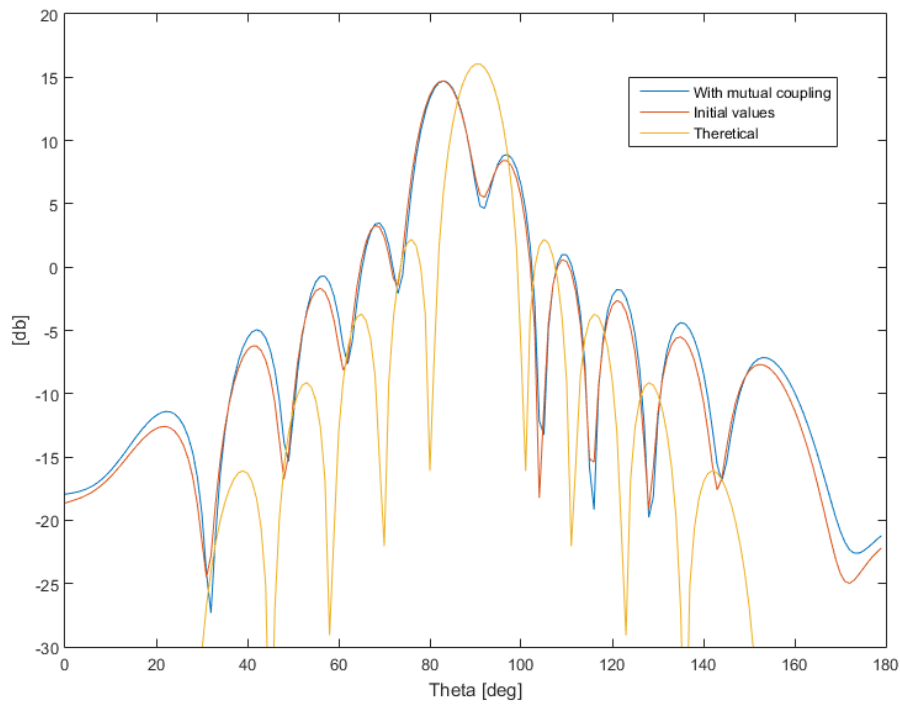*Figure 33. Radiation pattern at 10.2 GHz*

Figure 34. Radiation pattern at frequency 9.15 GHz

The radiation pattern at 10.2 GHz is in good agreement with the theory. The gain of the antenna is 16 dB and the first side lobe is at 2.2 dB which results in a -13.8 dB side lobe level. As the theory predicted the radiation pattern is narrow in one plane, at constant Φ the half power beam width is only 8.4 degrees but it is 83.0 degrees wide in the other plane. The radiation pattern at 9.15 GHz is distorted, the main lobe is inclined by 10 degrees and the biggest side lobe is only 6 dB below the level of the main lobe. It is also visible from Figure 33. that the mutual coupling has no major effect on the radiation pattern.
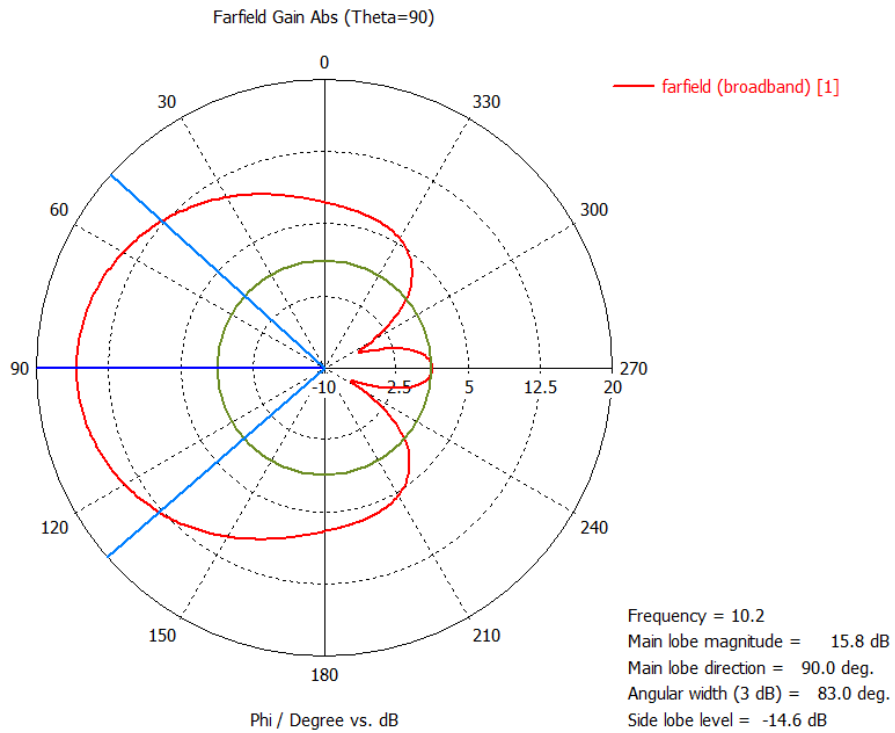
Farfield Gain Abs (Theta=90)

Frequency = 10.2
Main lobe magnitude =   15.8 dB
Main lobe direction =   90.0 deg.
Angular width (3 dB) =   83.0 deg.
Side lobe level = -14.6 dB

Phi / Degree vs. dB

Figure 35. Radiation pattern at phi=90°

7.2. Low side lobe level antenna

The second simulated antenna was made with the intention to achieve the side lobe level of -20 dB. To do this the cosine aperture distribution has been selected from Figure 26. which in theory should result in a -23 dB SLL. The slot voltage distribution has been calculated as shown in Figure 36. The red crosses mark the position of the slot's center and the corresponding slot voltage has been assigned to each slot. The resulting slot dimensions are presented in Table 6.

Slot	1	2	3	4	5	6	7	8
Offsets [mm]	1,8928	2,0179	2,7057	2,9142	2,9142	2,7057	2,0179	1,8928
Length [mm]	15,556	15,570	15,664	15,698	15,698	15,664	15,570	15,556

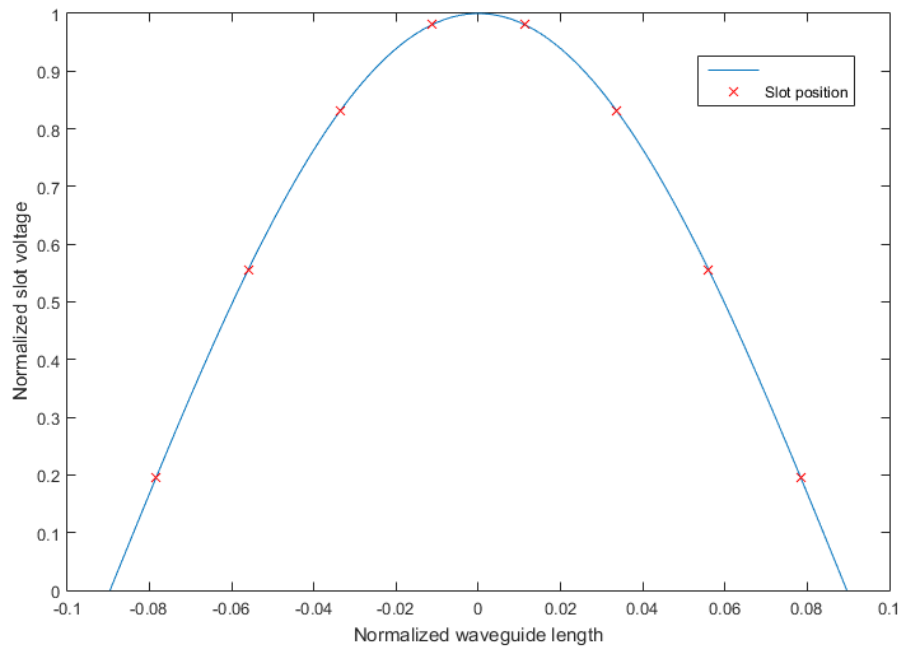*Table 6. Slot dimensions of the side lobe level antenna*

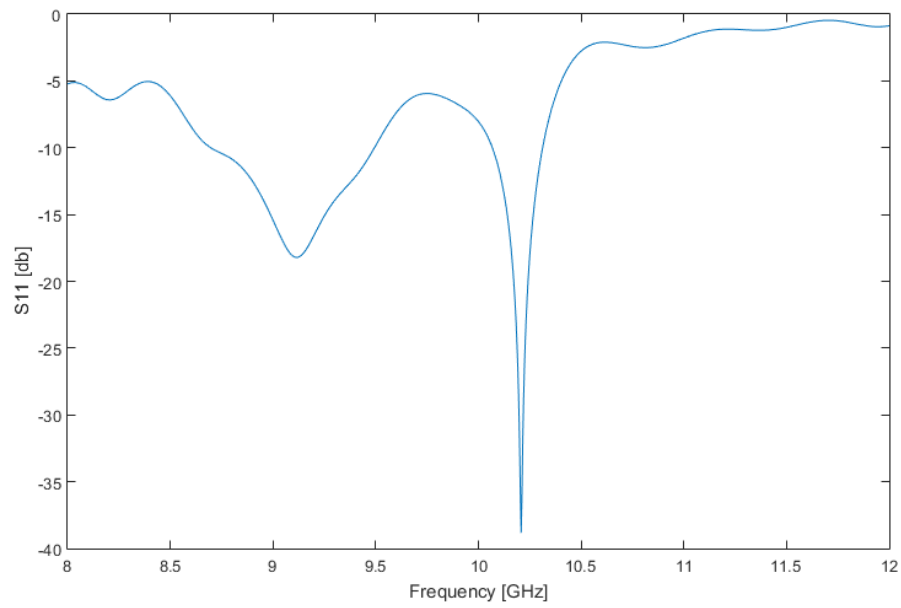*Figure 36. Cosine slot voltage distribution*

Figure 37. s11 parameter of the side lobe level antenna

Figure 37. shows a the s_{11} parameter of the antenna. There is a perfect match at frequency 10.2 GHz, but just as in the previous case the antenna is well matched at frequency 9.15 GHz.

The radiation pattern is compared with the theoretical pattern in Figure 38. The antenna has higher maximal gain with 15.91dB than predicted and lower SLL. The highest side lobe is -2.99 dB which results in a -18.9 dB side lobe level which is 1.1 dB shy of the requested value. The two antennas radiation pattern is compared in Figure 40. The two gains are nearly the same, but the side lobe suppression due to the used cosine voltage distribution is clearly visible.
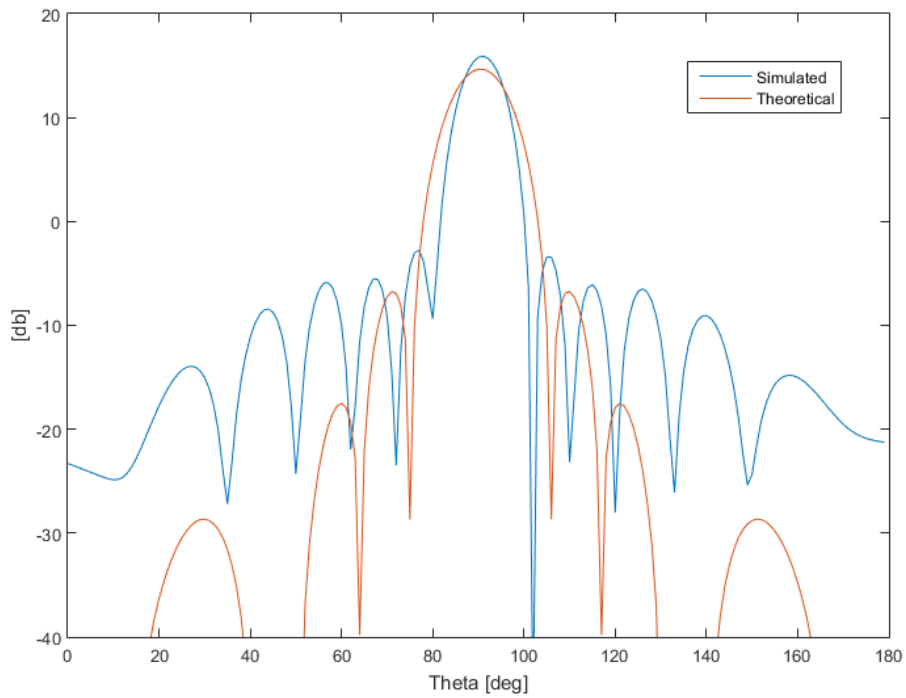

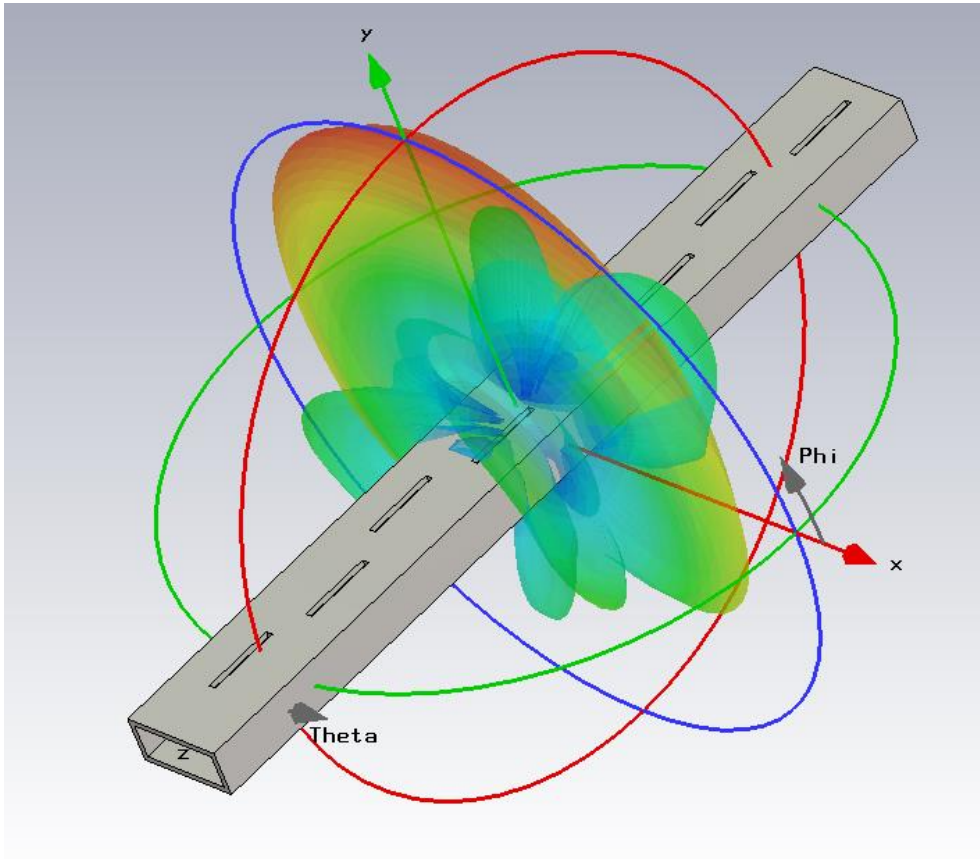*Figure 38. Radiation pattern of the side lobe level antenna*

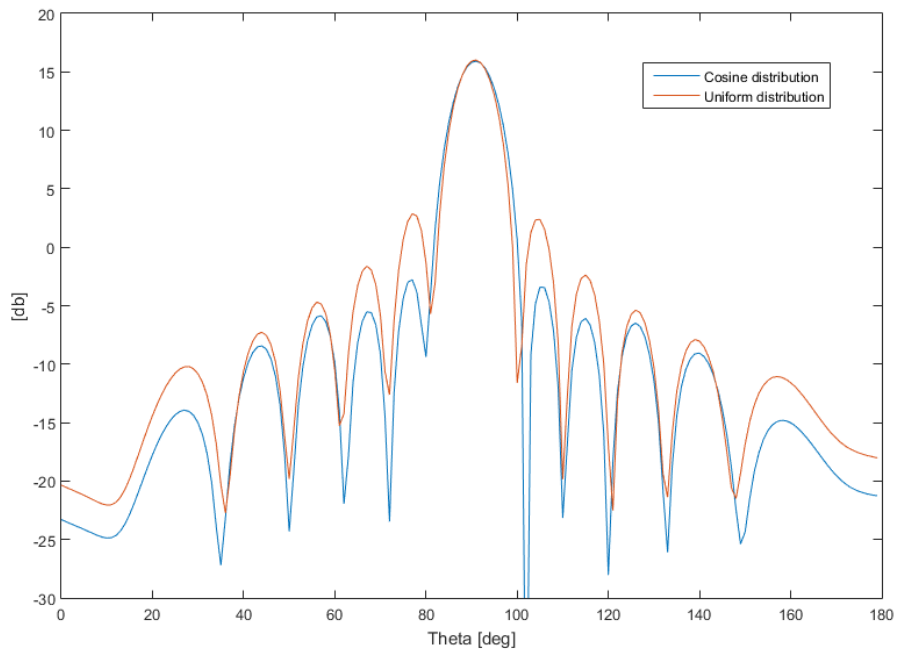*Figure 39. 3D radiation pattern of the side lobe level antenna*

Figure 40. Comparison of the radiation patterns

8.   Conclusion

The first goal of this thesis was to analyze the radiation of a longitudinal slot in the broad wall of the waveguide and examine the effect of slot dimensions and offset on the conductance of the slot and compare the simulated results to the theoretical equations. The second goal was to describe the design procedure of the waveguide slot array antennas and implement the procedure in MATLAB. Furthermore two antennas have been designed, one with maximal gain and the other with a defined side lobe level.

Firstly, the effect of waveguide wall width was inspected. The results confirmed that the theoretical equations were derived for infinitely thin wall. For thin waveguide wall the simulated and calculated values show good agreement, but for thicker wall the equations have to be multiplied by an appropriate constant to match the simulated values.

Secondly, the effect of slot width was observed. The simulations showed that this dimension has a negligible effect on the impedance of the slot and on the resonant frequency, therefore the recommended value can be used.

Thirdly, the effect of slot length was analyzed. This parameter mainly influences the resonant frequency. Moreover from the results it is also visible that the impedance of the slot also changes with the length.

A design guideline is presented, according to which two simple antennas were designed in CST Microwave studio. The smaller antenna's radiation pattern is a little inclined and the main beam is wide in both planes. According to expectations the four slot antenna has higher gain and better sector-shaped radiation pattern, but the impedance matching is very poor due to the mutual coupling between slots.

In the second half of the thesis the design equations have been described in detail. Moreover a step-by-step guide is presented on how to design a slot array antenna. The process starts with collecting the data for Stegen curves either from measurements or simulations or by using the method of moments. The second step involves choosing the number of slots and calculating the slot voltage distribution from the required radiation pattern. After this the initial slot offsets and lengths may be calculated which is followed by determining the mutual coupling between the slots. With the knowledge of these values the search for improved slot dimensions can be undertaken by detuning the slots from self-resonance to compensate the mutual coupling effect. This last two steps may be repeated until the difference between them is smaller than the matching tolerance.

The described process has been implemented in MATLAB and it was tested on a small 4 array slot antenna. The calculated slot dimension showed a good agreement with the values from Elliott, but due to the inaccurate Stegen curves the simulated results were distorted.

In the final chapter two 8 slot array antennas have been designed and simulated. On the first one the effect of the mutual coupling is clearly shown as the improved slot dimension resulted in a 20dB better impedance match. The radiation patterns of the maximal gain antenna showed good agreement with the theory. The second antenna was intended to have a better side lobe level and a nearly 6 dB improvement was achieved due to the used slot voltage distribution.

9. References

[1] Johnson, R. C., "Antenna Engineering Handbook, Third Edition", McGraw-Hill, 1993

[2] Elliott, R. S., ''Antenna Theory and Design", IEEE Press Series in Electromagnetic Wave Theory, 2003.

[3] Bevelacqua, P. J., "Antenna Theory Basics", http://www.antenna-theory.com/

[4] Orfanidis, S. J., "Electromagnetic Waves and Antennas", http://www.ece.rutgers.edu /~orfanidi/ewa/

[5] Stevenson, A. F., "Theory of slots in rectangular waveguides", Journal of Applied Physiscs, vol. 19, pp. 24-38; Jan. 1948

[6] Elliott, R.S.; Kurtz, L., "The design of small slot arrays," *Antennas and Propagation, IEEE Transactions on* , vol.26, no.2, pp.214,219, Mar 1978

[7] Tai, C. T., Jasik, H. "Antenna Engineering Handbook", McGraw-Hill, 1961

[8] Computer Simulation Technology, available from www: https://www.cst.com/

[9] WADE, P., "Microwave Antenna book", http://www.qsl.net/n1bwt/ch7_part1.pdf

[10] R. Elliott, "An improved design procedure for small arrays of shunt slots," in *IEEE Transactions on Antennas and Propagation*, vol. 31, no. 1, pp. 48-53, Jan 1983.

[11] Lo, Yuen T., and S. W. Lee. Antenna Handbook: theory, applications, and design. Springer Science & Business Media, 2013.

[12] Orfanidis, Sophocles J. Electromagnetic waves and antennas. New Brunswick, NJ: Rutgers University, 2002.

[13] Josefsson, Lars G. "Analysis of longitudinal slots in rectangular waveguides." Antennas and Propagation, IEEE Transactions on 35.12 (1987): 1351-1357.

[14] Gatti, Roberto Vincenti, Roberto Sorrentino, and Marco Dionigi. "Equivalent circuit of radiating longitudinal slots in dielectric filled rectangular waveguides obtained with FDTD method." Microwave Symposium Digest, 2002 IEEE MTT-S International. Vol. 2. IEEE, 2002.

[15] Oraizi, Homayoon, and Mahmoud T. Noghani. "Design and optimization of nonuniformly spaced longitudinal slot arrays." Progress In Electromagnetics Research M 4 (2008): 155-165.

[16] Oraizi, Homayoon, and Mahmoud T. Noghani. "Design and optimization of linear and planar slot arrays on rectangular waveguides." Microwave Conference, 2008. EuMC 2008. 38th European. IEEE, 2008.

[17] Stegen, Robert J. Longitudinal shunt slot characteristics. No. HAC-TM-261. HUGHES AIRCRAFT CO CULVER CITY CA RESEARCH AND DEVELOPMENT DIV, 1951.